Columbia University
in the City of New York

DEPARTMENT OF CIVIL ENGINEERING

TRANSITION TEMPERATURES OF STRUCTURAL STEEL BEAMS WITH BUTT WELDED SPLICES.

By

WILLIAM J. KREFELD and GEORGE B. ANDERSON

Technical Report to Office of Naval Research and
Welding Research Council of the Engineering Foundation
Office of Naval Research Contract No-onr-271 - T.O. 7,
CU-1-53-ONR - 271-C.E.

OCTOBER — 1953

Columbia University
in the City of New York

DEPARTMENT OF CIVIL ENGINEERING

TRANSITION TEMPERATURES OF STRUCTURAL STEEL BEAMS WITH BUTT WELDED SPLICES.

By

WILLIAM J. KREFELD and GEORGE B. ANDERSON

Technical Report to Office of Naval Research and
Welding Research Council of the Engineering Foundation
Office of Naval Research Contract No-onr-271 - T.O. 7,
CU-1-53 ONR - 271-C.E.

OCTOBER — 1953

Prepriated from the November 1953 Issue
of the Welding Research Supplement.

Issued September 1953
No. of Copies Indicated 110

DISTRIBUTION LIST
FOR
UNCLASSIFIED Technical and Final Reports Issued Under
Office of Naval Research Project NR 064-150, Contract N6onr 271(07)

Administrative, Reference and Liaison Activities of ONR

Chief of Naval Research
Department of the Navy
Washington 25, D. C.
Attn: Code 423 (1)
Code 438 (2)

Director
Naval Research Laboratory
Washington 25, D. C.
Attn: Tech. Info. Officer (6)
Technical Library (1)
Mechanics Division (2)
Metallurgy Division (1)

Commanding Officer
Office of Naval Research
Branch Office
346 Broadway
New York 13, New York (1)

Commanding Officer
Office of Naval Research
Branch Office
John Crerar Library Bldg.
86 East Randolph Street
Chicago, Illinois (1)

Commanding Officer
Office of Naval Research
Branch Office
1030 Green Street
Pasadena, California (1)

Commanding Officer
Office of Naval Research
Branch Office
1000 Geary Street
San Francisco 24, California (1)

Commanding Officer
Office of Naval Research
Branch Office, London
Navy #100, FPO
New York, N. Y. (5)

Office of Technical Services
Department of Commerce
Washington 25, D. C. (1)

Armed Services Technical
Information Agency
Document Service Center
Knott Building
Dayton 2, Ohio (5)

Department of Defense
Other Interested Government Activities

GENERAL

Research and Development Board
Department of Defense
Pentagon Building
Washington 25, D. C.
Attn: Library (Code 3D-1075) (1)

Armed Forces Special Weapons Project
P. O. Box 2610
Washington 25, D. C.
Attn: Blast & Shock Branch (1)

ARMY

Chief of Staff
Department of the Army
Research and Development Division
Washington 25, D. C.
Attn: Chief, Research & Development (1)

Office of the Chief of Engineers
Assistant Chief for Works
Department of the Army
Bldg. T-7, Gravelly Point
Washington 25, D. C.
Attn: Structural Branch
(R. L. Bloor) (1)

Office of the Chief of Engineers
Asst. Chief for Military Construction
Department of the Army
Bldg. T-7, Gravelly Point
Washington 25, D. C.
Attn: Structures Branch
(H. F. Carey) (1)

ARMY (Continued)

Engineering Research &
Development Laboratory
Fort Belvoir, Virginia
Attn: Structures Branch (1)

The Commanding General
Sandia Base, P. O. Box 5100
Albuquerque, New Mexico
Attn: Col. Canterbury (1)

Office of Chief of Ordnance
Research & Development Service
Department of the Army
The Pentagon
Washington 25, D. C.
Attn: ORDTB (2)

Office of Ordnance Research
2127 Myrtle Drive
Duke Station
Durham, North Carolina (1)

Commanding Officer
Watertown Arsenal
Watertown, Massachusetts
Attn: Laboratory Division (1)

NAVY

Chief, Bureau of Ships
Department of the Navy
Washington 25, D. C.
Attn: Code 318 (1)
Code 343 (1)
Code 423 (1)
Code 440 (1)
Code 442 (1)

Director and Commanding Officer
David Taylor Model Basin
Washington 7, D. C.
Attn: Structural Mechanics Div. (1)
High Speed Dynamics Br. (1)

Director
Materials Laboratory
New York Naval Shipyard
Brooklyn 1, New York (2)

Chief, Bureau of Ordnance
Department of the Navy
Washington 25, D. C.
Attn: Technical Library
Code AD-3 (1)

Superintendent
Naval Gun Factory
Washington 25, D. C. (1)

Commanding Officer
Naval Ordnance Laboratory
White Oak
Silver Spring, Maryland
Attn: Code W (1)
Code T (1)

Commanding Officer
Naval Ordnance Test Station
Inyokern, California
Attn: Scientific Officer (1)

Commanding Officer
Naval Ordnance Test Station
Underwater Ordnance Division
Pasadena, California
Attn: Structures Division (1)

Chief, Bureau of Aeronautics
Department of the Navy
Washington 25, D. C.
Attn: TD-41 (1)

Chief, Bureau of Yards and Docks
Department of the Navy
Washington 25, D. C.
Attn: Code P-314 (1)

Officer in Charge
Naval Civil Engineering Research
and Evaluation Laboratory
U.S. Naval Station
Port Hueneme, California (2)

Superintendent
U.S. Naval Post Graduate School
Monterrey, California (1)

Commander
U.S. Naval Proving Grounds
Dahlgren, Virginia (1)

AIR FORCES

Director of Intelligence
Headquarters, U.S. Air Force
Washington 25, D. C.
Attn: Air Targets Division -
PV Branch (1)

AIR FORCES (Continued)

Commanding General
Air Materiel Command
Wright-Patterson Air Force Base
Dayton, Ohio
Attn: Materials Laboratory (1)

Commanding General
Air Research and Development Command
P.O. Box 1395
Baltimore 3, Maryland
Attn: RDDN (1)

OTHER GOVERNMENT AGENCIES

Director
National Bureau of Standards
Washington, D. C.
Attn: Mr. Sam Levy (1)

Commandant
U.S. Coast Guard
1300 E Street, N.W.
Washington 25, D. C.
Attn: CDR D. B. Henderson
Secy, SSSC (1)

U.S. Maritime Commission
Technical Bureau
Washington, D. C.
Attn: Mr. V. Russo (1)

National Science Foundation
Cosmos Club
1520 H Street, N. W.
Washington, D. C. (1)

National Academy of Sciences
2101 Constitution Avenue
Washington 25, D. C.
Attn: Dr. Finn Jonassen (1)

Contractors and Other Investigators
Actively Engaged in Related Research

Professor Lynn Beedle
Fritz Engineering Laboratory
Lehigh University
Bethlehem, Pennsylvania (1)

Dr. Hans H. Bleich
Department of Divil Engineering
Columbia University
New York 27, New York (1)

Contractors (Continued)

Professor T. J. Dolan
Department of Theoretical and
Applied Mechanics
University of Illinois
Urbana, Illinois (1)

Professor D.C. Drucker, Chairman
Division of Engineering
Brown University
Providence 12, Rhode Island (1)

Professor A. M. Freudenthal
Department of Civil Engineering
Columbia University
New York 27, New York (1)

Dr. R. J. Hansen
Massachusetts Institute of Technology
Department of Civil & Sanitary
Engineering
Cambridge 39, Massachusetts (1)

Dr. N. J. Hoff, Head
Department of Aeronautical Engineering
and Applied Mechanics
Polytechnic Institute of Brooklyn
99 Livingston Street
Brooklyn 2, New York (1)

Dr. W. H. Hoppmann, II
Department of Applied Mechanics
John Hopkins University
Baltimore, Maryland (1)

Professor Bruce G. Johnston
University of Michigan
Ann Arbor, Michigan (1)

Professor W. J. Krefeld
Department of Civil Engineering
Columbia University
New York 27, New York (10)

Professor B. J. Lazan
Department of Materials Engineering
University of Minnesota
Minneapolis, Minnesota (1)

Dr. E. H. Lee
Division of Applied Mathematics
Brown University
Providence, Rhode Island (1)

Contractors (Continued)

Professor George H. Lee
Department of Mechanics
Rensselaer Polytechnic Institute
Troy, New York (1)

Professor J. Marin
Pennsylvania State College
State College, Pennsylvania (1)

Professor R. D. Mindlin
Department of Civil Engineering
Columbia University
632 West 125th Street
New York 27, New York (1)

Dr. N. M. Newmark
Department of Civil Engineering
University of Illinois
Urbana, Illinois (1)

Dr. R. P. Petersen
Director, Applied Physics Division
Sandia Laboratory
Albuquerque, New Mexico (1)

Dr. S. Raynor
Armour Research Foundation
Illinois Institute of Technology
Chicago 16, Illinois (1)

Dr. Daniel T. Sigley
Applied Physics Laboratory
John Hopkins University
8621 Georgia Avenue
Silver Spring, Maryland (1)

Dr. C. B. Smith
College of Arts and Sciences
Department of Mathematics
Walker Hall
University of Florida
Gainesville, Florida (1)

Professor C. R. Soderberg
Massachusetts Institute of Technology
Cambridge, Massachusetts (1)

Members
Columbia Project Committee
(one copy each) (12)

Transition Temperatures of Structural Steel Beams with Butt-Welded Splices

William J. Krefeld and George B. Anderson

Technical Report to the Office of Naval Research and the Welding Research Council of the Engineering Foundation. Office of Naval Research Contract N6-onr-271-T.O.7 CU-1-53-ONR-271-C.E. 1953

Preprinted from the November 1953 issue of the Welding Research Supplement

Transition Temperatures of Structural Steel Beams with Butt-Welded Splices

An investigation of the resistance of butt-welded and unwelded structural beams to impact loads at low winter temperatures including relative behavior of semikilled and fully killed steels, low-hydrogen versus ordinary electrodes, with and without cope holes

by William J. Krefeld and George B. Anderson

Scope

This investigation was primarily concerned with the resistance and transition temperatures of structural steel beams, composed of semikilled and fully killed steels and fabricated with butt-welded splices. Static and impact tests on 16-in. WF 71-lb beams, in addition to confirming the favorable effect of aluminum deoxidation in lowering the transition temperature of the as-rolled base metal indicated by Charpy tests, furnished information on the relative behavior of the two grades of steel with splices as-welded, welded and "stress relieved" and when welded with preheat. The influence of these treatments was evaluated by increment drop impact tests on beams welded with E6011 and E6020 electrodes. Similar supplementary tests on beams composed of both steels when welded with low-hydrogen electrodes as-welded and with preheat, furnish comparative data. Other data deals with the character of fracture and the effect of flame-cut holes in the beam web. The influence of a sharp notch at a critical location in an unwelded beam and the tendency of crack propagation are indicated by the results of supplementary tests.

This investigation was conducted by the Civil Engineering Research Laboratories of Columbia University under the joint sponsorship of the Office of Naval Research, Contract No. N6-onr-271, T.O. 7 and the Welding Research Council of the Engineering Foundation, under direct supervision of the Structural Steel Research Committee of the Welding Research Council.

INTRODUCTION

THE present investigation is an extension of previous experimental studies[1] of the behavior of beams with butt-welded splices under impact, which dealt with the possible cumulative effect of residual stresses at strain rates associated with impact loading. Residual stresses of considerable magnitude were found in the vicinity of the weld,[2] which lowered the apparent proportional limit. There was no evidence of any adverse effect upon the ultimate behavior of the beams, which developed refusal loads by lateral buckling or web crippling, without fracture, at the test temperature of +70° F. A limited number of tests conducted at −40° F, however, resulted in complete brittle fractures through the welds.

The investigation here recorded was intended to determine the low temperature performance of butt-welded beams under impact loading, which afforded a comparison of the relative suitability of two grades of structural steel and the influence of thermal treatments of the weldments. The testing temperatures ranged from +70° F to −115° F which permitted determination of the critical temperature of transition from the normal ductile type of buckling failure to failure by brittle fracture.

The beams were rolled from heats of semikilled and silicon-aluminum fully killed steels. Charpy and Kahn tests indicated lower transition temperatures for the fully killed as-rolled base metal. In order to determine the effects of welding procedure, tests were conducted on beam specimens in which the weldments, made with E6011 and E6020 electrodes, represented three treatments; namely, (1) as-welded, (2) welded and stress relieved by postheating the entire welded beam to 1150° F for 2 hr, followed by furnace cooling to 500° F and final air cooling and (3) welded after preheating, with interpass temperatures of 350–400° F. Supplementary specimens of both base metals were fabricated with low-hydrogen (E6016) electrodes, both with and without preheat.

The low-temperature properties indicated by laboratory tests are influenced by the method of loading, geometry of the specimens and associated strain rate. In dealing with the material in a rolled section, the results of small-scale tests are further complicated by the variation of properties according to location in the sec-

William J. Krefeld is Professor of Civil Engineering, Director of Research, Materials Laboratory, Columbia University, New York, N. Y., and **George B. Anderson** is Research Associate, Department of Civil Engineering, Columbia University, New York, N. Y.

Technical Report to the Office of Naval Research and the Welding Research Council of the Engineering Foundation. Office of Naval Research Contract N6-onr-271-T.O. 7, CU-1-53-ONR-271-C.E. 1953

Table 1—Chemical Analysis of Structural Steel Beams (Bethlehem Steel Co.)

	C	*Mn*	*P*	*S*	*Si*	*Ni*	*Cr*	*Mo*	*Cu*	*Sn*	N_2	*Al*
Semikilled steel (Heat 34J333)												
Ladle	0.22	0.58	0.017	0.031	0.06	0.06	0.06	0.03	0.14	0.012	...	...
Check	0.21	0.57	0.021	0.031	0.01	0.04	0.06	Nil	0.14	0.01	0.005	0.006
Fully killed steel (Heat 35J272)												
Ladle	0.19	0.72	0.023	0.031	0.23	0.07	0.04	0.03	0.14	0.017	...	...
Check	0.19	0.72	0.023	0.029	0.21	0.05	0.02	Nil	0.16	0.01	0.006	0.047

tion. Similarly, a comparison of the influence of welding involves the relative cooling rates of large and small specimens. The interpretation of test results from full size weldments, though satisfying with respect to particular design application, has limitations for generalized correlation purposes due to the influence of individual fabrication requirements, not otherwise reproducible. For example, the beam specimens used in the present studies, butt welded according to a specified procedure, include holes in the web adjacent to both flanges to facilitate the welding of the flanges. These flame-cut holes introduce local strain concentrations and indeterminate strain rates. In effect, the specimen includes an internal notch, complicated by the fact that the web weld terminates at this notch. Nevertheless, these beams represent a practical type of welded splice, whose behavior is of interest to the designing engineer, and afford comparison of the relative suitability of the two steels and welding treatments under the same design conditions. A limited number of additional comparative tests were made on a modified splice design eliminating the web holes.

It was considered desirable to proceed first with a series of "static" load tests with the hope of determining the relative low-temperature performance without elaborate instrumentation. However, the tests made on beams of both steels and different treatments at −115° F were inconclusive because all failures were caused by buckling. It was apparent that the determination of the relative tendency to failure by brittle fracture required either lower testing temperatures or higher strain rates. The lowering of the temperature below −115° F would have required a more elaborate refrigeration procedure. The testing under higher strain rates by increment drop impact tests were adopted for further studies. The testing procedures and results of both "static" (low strain rate) and impact tests are recorded in the following discussion.

MATERIALS

The beams used for these tests were 16-in. WF 71-lb sections, prepared by butt welding two 7-ft lengths to form a beam 14 ft long, for tests on a 12-ft span. The materials from which these beams were rolled represented two types of steel; namely, ASTM A7–46, semikilled steel (Heat 34J333) and ASTM A7–46, silicon-aluminum fully killed steel (Heat 35J272). Through the cooperation of the Bethlehem Steel Co., a complete history of the manufacture, fabrication and physical properties was recorded. A summary of the melting practice, mill practice and fabrication procedures as reported by the manufacturer is given in the Appendix. These heats provided 50 semikilled and 100 fully killed beams, 14 ft long, for this investigation.

The reported chemical analysis for these two steels is shown in Table 1.

It was the intention, in planning these tests, to include structural grade steels having appreciable differences in low-temperature properties as indicated by

Table 2—Physical Properties

*Specimen location**	*Yield point, psi*	*Yield strength, psi*	*Tensile strength, psi*	*Elongation %, 8 in.*	*Elongation %, 2 in.*	*Bend*	*McQuaid-Ehn grain size*
Semikilled, as-rolled							
Web, 4 in. from centerline (Beth.)	37,260	37,580	63,380	27.5	47.5	OK	100%, 1–3
Web, 5 in. from centerline	35,250	35,250	63,500	28.9	50.0	...	
Web, 1 in. from centerline	38,600	38,350	65,100	29.3	48.5	...	
Flange, 2 in. from edge	36,400	36,400	63,800	29.6	52.0	...	
Semikilled, stress relieved							
Web, 4 in. from centerline (Beth.)	37,260	37,400	62,190	28.7	49.5	OK	100%, 1–3
Fully killed, as-rolled							
Web, 4 in. from centerline (Beth.)	41,540	41,670	69,530	25.0	44.5	OK	100%, 6–8
Web, 5 in. from centerline		38,900	65,300	29.0	45.0	...	
Web, 1 in. from centerline	41,800	42,500	66,800	27.0	47.0	...	
Flange, 2 in. from edge	39,300	39,500	66,900	28.0	51.0	...	
Fully killed, stress relieved							
Web, 4 in. from centerline (Beth.)	43,920	44,190	67,160	27.5	49.0	OK	100%, 6–8
Web, 5 in. from centerline		38,600	66,500	26.4	49.0	...	
Web, 1 in. from centerline	42,700	42,700	68,300	26.8	46.5	...	
Flange, 2 in. from edge	40,000	40,500	66,700	29.0	54.5	...	

* Refers to location of center of 2-in. wide coupon; toe of fillet 6⅞ in. from center of web. All tests at +70° F.
REMARKS: Microstructure of both steels reported by manufacturer to be banded Sorbitic Pearlite and Ferrite.

conventional small specimen tests in order that these identifying properties might be compared with the behavior of full-scale weldments. The properties recorded included the standard tensile properties of various locations, Charpy V notch and keyhole notch impact transition data, and the results of Kahn tear tests. These properties were determined from specimens taken from the rolled beams and represented both as-rolled material and material after stress-relieving treatment at 1150° F for $\frac{1}{2}$ hr. Additional static tensile tests were made to determine the effect of temperature.

Table 2 records the results of standard tension tests on flat specimens taken from various locations of the web and flange. These results indicate higher yield point and ultimate strength for the fully killed steel, without appreciable difference in elongation. The yield strength was lowest for specimens taken from the web adjacent to the fillet for both steels. The properties do not appear to be appreciably affected by stress-relieving treatment.

Comparative Charpy and Kahn tests were made at the mill on specimens taken from the web about midway between the fillet and centerline. Because of the character of fracture of the welded beams it was of interest to investigate the variation of low-temperature properties by additional Charpy tests on specimens taken from the edge and center of the flanges and near the fillet and centerline of the web. All specimens were taken in the direction of rolling with notches on sides perpendicular to the original surface. The results of the Charpy and Kahn tests are shown in Figs. 1-5.

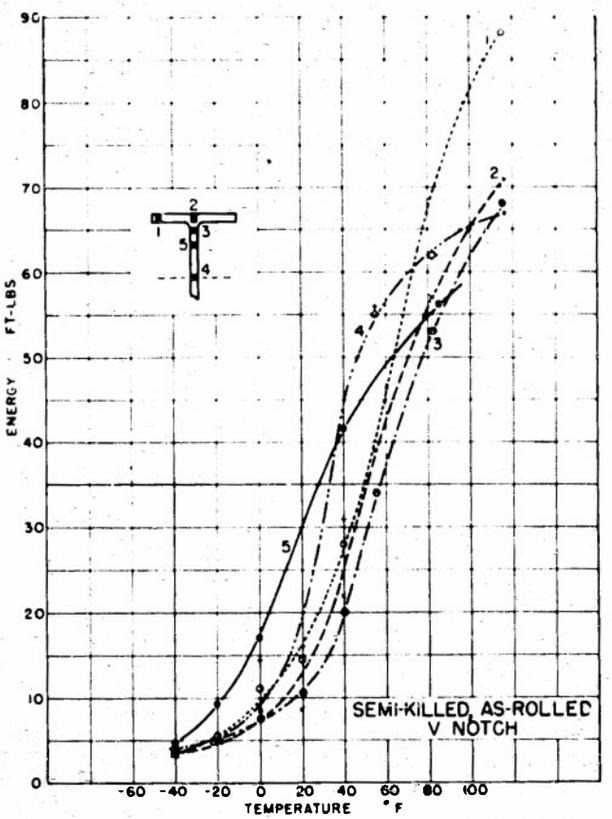

Fig. 1 Charpy impact test results

These curves indicate that the abrupt decrease in fracture energy occurs at higher temperatures for material taken near the fillet in both the flange and web. The curves for materials taken from the web between the fillet and centerline show intermediate energy values except that in all cases Curve 5 according to data submitted in the mill report shows considerably lower energy absorption at the higher temperatures. This may be a machine effect, possibly due to relative rigid-

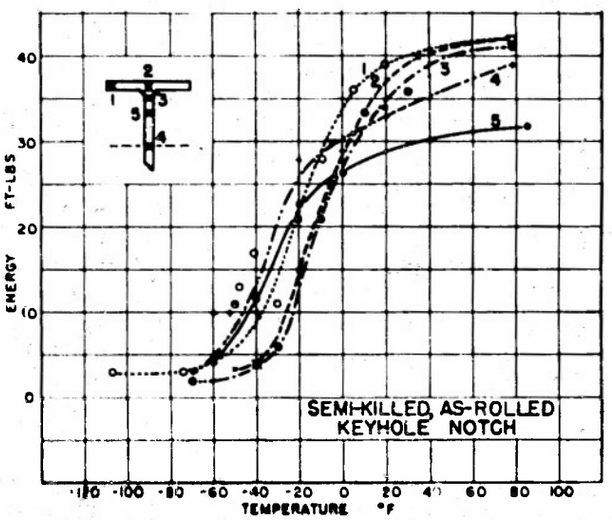

Fig. 2 Charpy impact test results

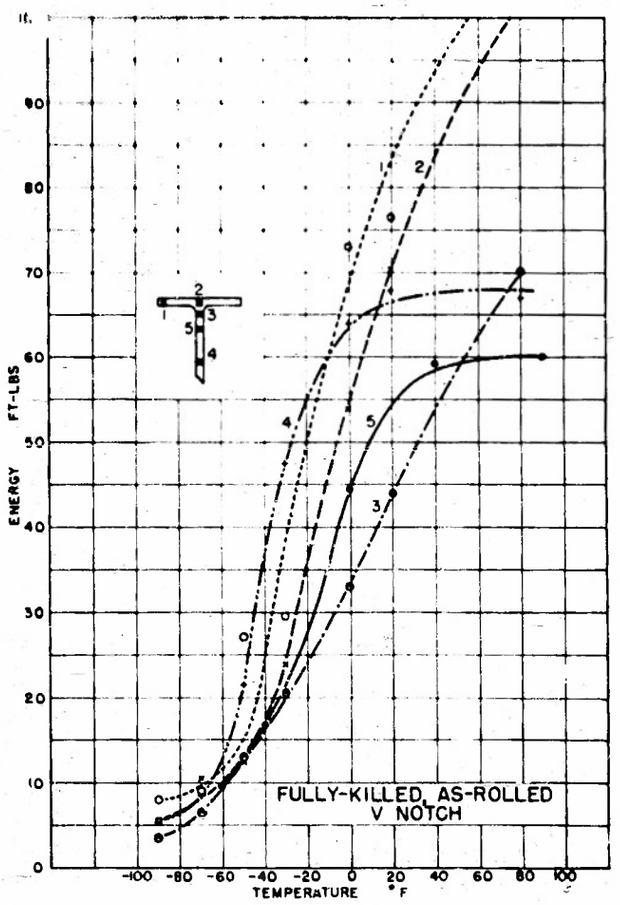

Fig. 3 Charpy impact test results

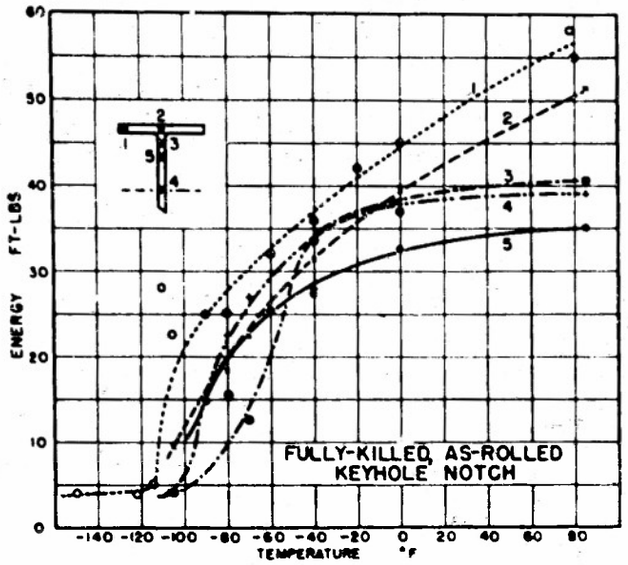

Fig. 4 Charpy impact test results

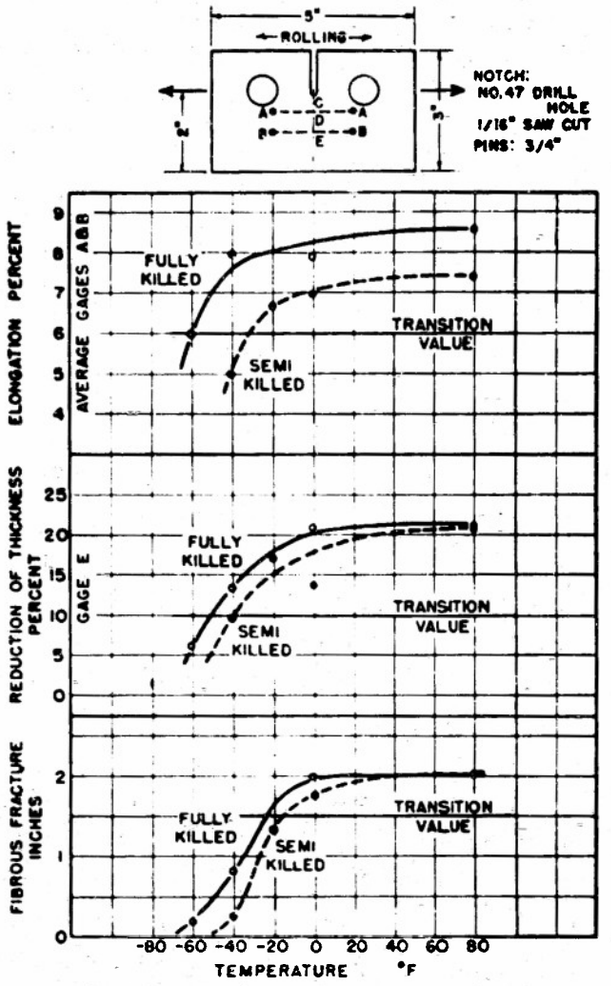

Fig. 5 Kahn tear test results

ities of the machines or supports which would have less influence at the lower fracturing energies. The energy values at the higher temperatures are not significant.

The transition temperatures derived from the Charpy tests are shown in Table 3. These temperatures are arbitrarily based on the 10 and 20 ft-lb levels for the keyhole notch and on the 15 and 50 ft-lb levels for the standard V notch. (Values at a common 15 ft-lb level are given for comparison.) The tabulated values show considerable spread for both types of notch depending upon location of the specimen, amounting to about 20° F for the semikilled steel and about 40° F for the fully killed steel. Under these circumstances a definite value of transition temperature cannot be assigned to either as-rolled steel but comparisons can be made of values at similar locations in the beam. The fully killed steel has transition temperatures based on the criteria shown, about 50 to 75° lower than the semikilled steel depending on location. It is evident that the silicon-aluminum deoxidation has decreased the notch sensitivity.

The greater spread of values indicated for the fully killed steel, particularly when based on the higher energy level criterion, is perhaps due to the character of fracture. In this steel, the fractures included numer-

Table 3—Transition Temperatures, Charpy Tests

Steel	*Test*	*Transition temperature, criterion-energy level*	*Transition temperatures, ° F* — *Flange* — *Edge (1)*	*Center (2)*	*Web* — *Near fillet (3)*	*Center (4)*	*¼ points* (5)*
Semikilled							
As-rolled	Charpy keyhole	20 ft-lb	22	−13	−11	−30	−25
As-rolled		10 ft-lb	−38	−26	−23	−46	−44
Stress relieved		20 ft lb					−22
As-rolled†		15 ft-lb	−29	−20	−18	−37	−34
As-rolled	Charpy V notch	50 ft-lb	+64	+70	+78	+47	+63
As-rolled		15 ft-lb	+17	+25	+33	+14	−4
Stress relieved		50 ft-lb					+60
Fully-Killed							
As-rolled	Charpy keyhole	20 ft-lb	−102	−79	−60	−84	−79
As-rolled		10 ft lb	−112	−103	−80	−95	−100
Stress relieved		20 ft-lb					−70
As-rolled†		15 ft-lb	−108	−93	−69	−90	−90
As-rolled	Charpy V notch	50 ft lb	−19	−5	+32	−26	+10
As-rolled		15 ft-lb	−50	−45	−42	−57	−45
Stress relieved		50 ft-lb					+25

* According to Bethlehem Steel Co. mill report data.
† For comparison with V notch at same energy level.

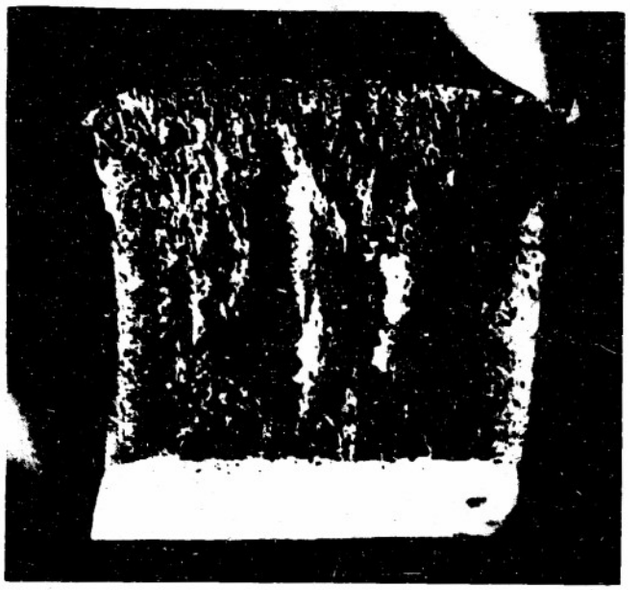

Plate 1 Fracture of Charpy specimen showing fissure

ous fissures which opened perpendicular to the direction of the notch. These fissures were found in all the fibrous fractures (higher temperatures), one of which is shown in Plate 1. In the intermediate transition range some fissures opened across a granular area and the fracture became fibrous immediately adjacent to the fissure. Probably due to lack of lateral restraint caused by the opening of the fissure, a more ductile local fracture resulted. These fissures were most pronounced in specimens taken from the center of the web and only occasionally in fractures of specimens taken from the edge of the flange. At lower temperatures, mixed results from a group of specimens showed that the presence of fissures raised the energy value from 4 to 25 ft-lb. At higher temperatures no relative values are available since all specimens developed fissures, but the curves for both notches indicate that the energy values were lowered. This opposite effect of fissures on the energy absorbed when large plastic deformations were produced at these higher temperatures is perhaps due to the relative volumes of material subjected to plastic deformation in a laminated as compared to a solid section. As in a simple tension test, the length of specimen affected by the "necking" before fracture is less for specimens with smaller sections, represented in this case by the multiple laminations.

The results of Kahn tear tests included in the mill report are shown in Fig. 5 and a summary of recorded data and transition temperatures based on various criteria is shown in Table 4. These data include final elongation in 2 in. on gage lengths located $^1/_2$ and 1 in. from the notch, reduction of thickness at the notch and $^1/_2$ and 1 in. from the notch, and the depth of section showing fibrous fracture. The transition values selected for the various measurements indicated a favorable influence of deoxidation but the temperature differences are not as great as for the Charpy tests.

The effect of temperature on the tensile lower yield point is shown in Fig. 6. Here again the data are subject to variations due to location of the specimens. The specimens were machined from adjacent $^3/_4$-in. wide strips cut longitudinally from one flange, located $1^3/_8$

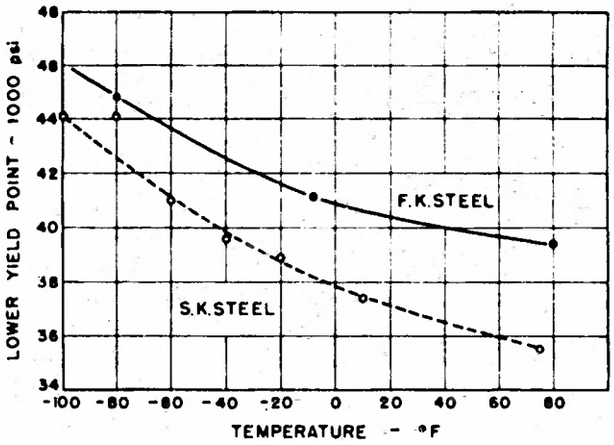

Fig. 6 Effect of temperature on lower yield point

Table 4—Summary of Kahn Tear Tests

Average values for specimens tested, according to Bethlehem Steel Co. report on materials—see Plate 5 for gage locations

No. specimens	*Temp., °F*	*Load, lbs*	*Elongation in 2 in., %* — *Gage A**	*Gage B†*	*Reduction in thickness, %, at: C*	*D*	*E*	*Type of fracture*
			Semikilled steel					
4	80	24,500	6.9	7.9	24.9	21.0	20.7	2-in. fibrous
2	0	26,300	7.0	7.0	24.1	18.1	13.8	$1^3/_4$-in. fibrous
3	−20	26,400	6.5	6.8	23.2	21.1	17.3	$1^1/_2$-in. fibrous
3	−40	26,900	5.5	4.5	25.2	15.6	9.6	$1^3/_4$-in. cryst.
			Fully killed steel					
3	80	28,030	8.0	9.3	24.8	21.8	21.3	2-in. fibrous
2	0	29,200	7.8	8.0	25.8	19.8	21.0	2-in. fibrous
3	−40	29,370	7.3	8.7	24.3	18.1	13.4	1.17-in. cryst.
3	−60	29,870	6.3	5.7	22.6	11.8	6.1	1.83-in. cryst.

Transition temperatures, °F, Kahn tear tests‡

Steel	*Fracture,*	*Elongation,*	*Reduction of thickness,*
Semikilled (AR)	−15	−30	−40
Fully killed (AR)	−23	−60	−50

* Gage line A-A located $^1/_2$ in. from center of hole.
† Gage line B-B located 1 in. from center of hole.
‡ Criteria: Elongation 6%, reduction of thickness 10%, fracture $1^1/_2$ in. fibrous.

and 2" in. from the flange edge. The specimens from the outside strip gave consistently higher yield points by about 2500 psi. The curves shown represent average values of 2 to 6 tests at a particular temperature. A few tension tests on the semikilled steel at −321° F showed a yield point of 116,000 120,000 psi. This value agrees reasonably well with a linear extension of the curve shown, to the lower temperature when the log of stress is plotted against 1/T, °R.

BEAM SPECIMENS

In preparation of the beams for butt welding, the ends of the web and flange to be welded were beveled by machine flame cutting to the dimensions shown in Fig. 7. The sections were mounted in a specially constructed positioning device which permitted rotation of the beams about their longitudinal axis, thus permitting welding in the flat position. The flanges were tack welded, about 1 in. at four points, located symmetrically about 2 in. from the edges, providing a root opening of 1/8 in. The tacks were placed on the outer flange surface and removed by gouging during the welding operation. Except for the special series welded with low hydrogen electrodes, the arc welds were made with 5/32-in. diam AWS-ASTM, E6011 welding rod for the root passes and 3/16-in. diam AWS-ASTM, E6020 rod for the subsequent passes. The web joint was welded first by one operator. The number of passes, sequence and direction of welding are shown in the Appendix summary of the mill report. The coped holes at the ends of the web weld were enlarged by flame cutting after completion of the weld to assure sound metal at the end of the web welds.

The surface condition of the finished welds was good. Some irregularities existed in the hand-cut cope holes. In order to place SR-4 strain gages on the curved edge of these holes, the inside curved edge was smoothed by hand filing. In later tests when gages were not used, the holes were similarly smoothed to ensure comparable test conditions. The alignment of the welded segments was good but due to normal tolerance variations a small relative axial rotation of the two segments or sloping flange surfaces made it necessary to machine tapering bearing plates at the end supports in order to erect the beams with web vertical. A lateral concavity of the outer flange surface also required grinding of these surfaces at the supports to provide flat bearings. These precautions were necessary in preparing the specimens for impact tests in order to avoid eccentric load with resulting lateral vibrations and other effects which influenced the deflection measurements.

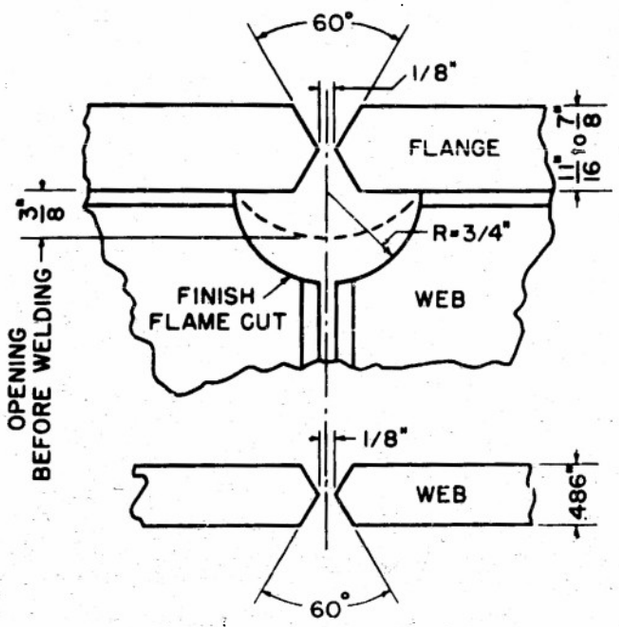

Fig. 7 Welding preparation details

TEST PROCEDURE

Static Tests

The beams were supported on heavy pedestals through 4-in. diam rollers between 2- x 12-in. plates at both ends, providing a 12-ft span. Load was applied through similar rollers at the third points of the span. Third-point loading was adopted to permit observation and measurement of strain distribution around the critical selection.

The entire beam, 14 ft long, was enclosed in an insulated chamber 18 in. wide, 28 in., high and 16 ft 8 in. long, inside. The chamber was composed of side, end, top and bottom sections with lapping joints, which were readily bolted together. The sections were made of sheet metal, enclosing a 3 in. thickness of insulation. Inside both ends of the chamber, a receptacle for dry ice was attached to the bottom section as shown schematically in Fig. 8. A blower with a 12-in. fan at both ends furnished an air stream through the dry ice receptacle and the insulated enclosure. This air stream returned to the blower through ducts incorporated in the sides of the chamber, exhausting the air from ports in the bottom of the side panels near midspan. The system thus circulated cooled air along each half of the beam. The rate of cooling depended upon the volume of dry ice used and velocity of the air stream. The beams, weighing 1000 lb, were cooled from +70 to −115° F in from 4 to 5 hr.

The supporting pedestals were insulated by similar panels. The openings in the top of the chamber for the third-point loading jig were sealed with flexible boots consisting of rubberized fabric and insulating wool, and the distributing beam was similarly insulated to reduce heat conduction to the cooling chamber.

The temperature of the beam was measured by copper-constantan thermocouples held in small drilled holes with solder. Temperature stations were located on both top and bottom flanges near the third points of the span and additional couples in the air stream at the ends were used for control purposes. The temperatures after a short stabilizing period were quite uniform, with only small differences between the upper and lower flanges. The test assembly was similar to that used for

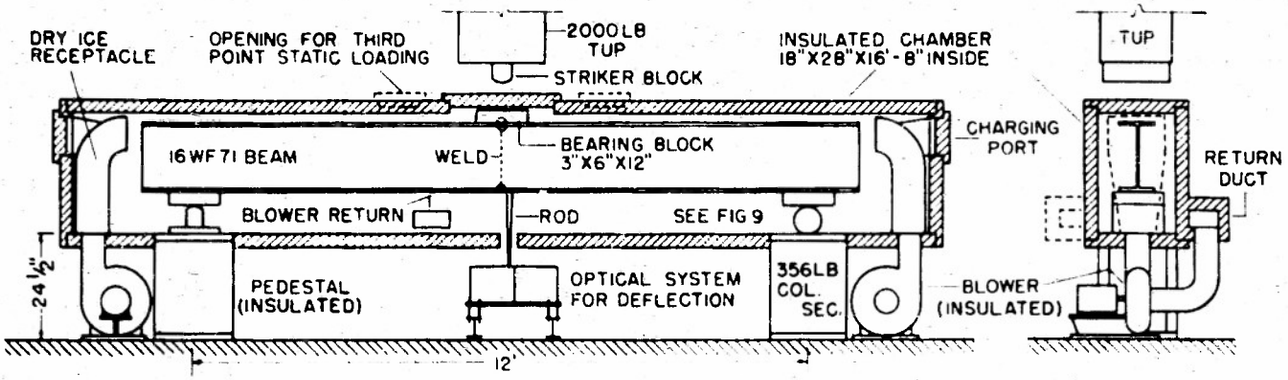

Fig. 8 Assembly for impact test

the impact tests shown in Fig. 8 with the exception of the third-point loading jig.

In order to measure the progress and distribution of strains across the section, SR-4 electric strain gages were placed longitudinally along the centerline of the weld after grinding the surface smooth, on the web and flange, and inside the cope holes. Gages were also placed at adjacent sections along the flanges. The center deflection of the lower flange was measured by reference to side bars attached on both sides to pins through the web over the supports. Attachment of the recording dial to a rod welded to the lower flange at midspan, and a yoke extension from the reference bars permitted readings outside the cooling chamber. Due to limited accessibility during the low-temperature tests, only midspan deflections were measured.

In order to compare the structural yield points, "refusal" loads and general load-deflection behavior of beams having different base metal properties and unknown effects of welding, it was desirable to maintain a constant loading rate. Due to interruption of loading for strain recording, inspection and necessary adjustments it was not possible to maintain constant loading conditions, particularly in the plastic range. It was possible, however, to reduce the observed load-deflection data to comparable curves at the same loading or deflection rates by the following procedure.

After the proportional limit was exceeded, as evidenced by the deflection increments, the loading which was applied at a convenient rate, was interrupted at various values of initially applied load and the deflection was maintained constant by readjustment of load by the testing machine as necessary. The increments of load or deflection between such interruptions were determined arbitrarily to give sufficient points for the derived curves. The load adjustments to maintain constant deflection—largely a machine effect—were small and intermittent. At each of the initially applied load increments, the decrease of load at constant deflection was recorded with time. Curves representing the decrease of load vs. time were called the "drop-off" or relaxation curves. At any interval of time after load application and stopping the machine, the instantaneous load was recorded as Pi. Then the rate of relaxation, dPi/dt was found from the relaxation curves at various values of Pi. A curve representing Pi vs. dPi/dt was plotted for each of the constant deflection increments. It was now possible to find values of Pi at selected relaxation

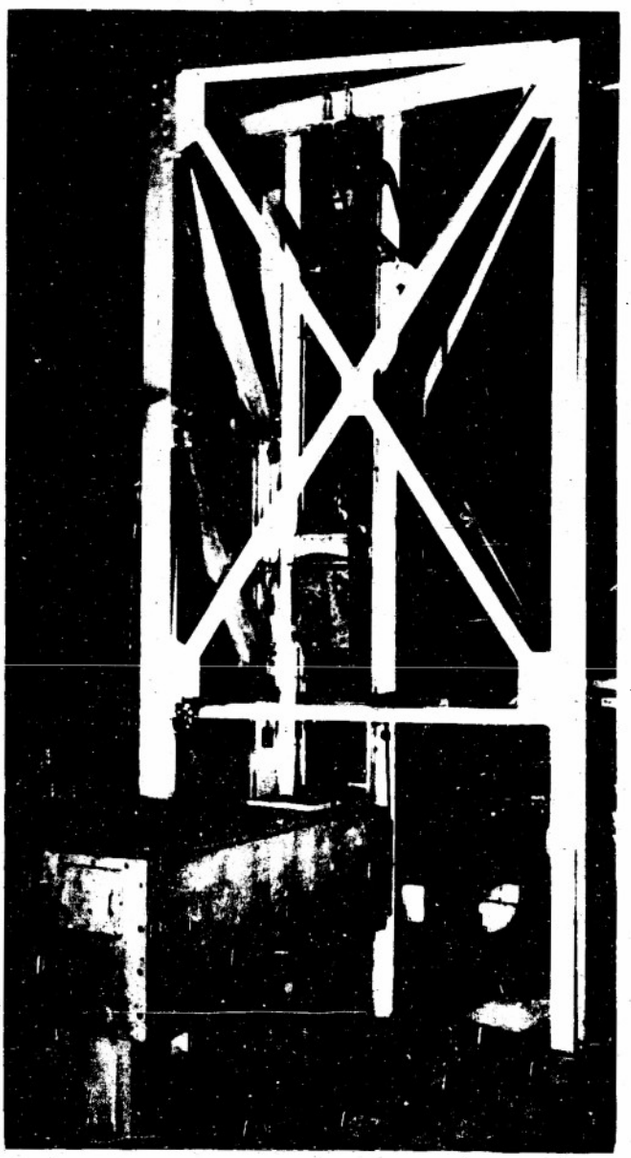

Plate 2 View of impact testing tower with beam specimen enclosed in cooling chamber

rates from each of the constant deflection curves. It will be noted that Pi represents the load resisted by the beam at a particular deflection when applied at the rate equal to the corresponding relaxation rate. Curves representing Pi vs. Δ can now be constructed for selected loading rates and the load-deflection data for the several beams can be compared with the same loading rate. The procedure is time consuming, if very low loading rates are used as the basis of comparison, because of the long period required for stabilization of the "drop-off" load. The highest rate is, of course, limited by the rate of initially applied load possible and controllable with the usual testing machine. However, the comparison can be made at relaxation rates which are reached in reasonably short holding times.

The effect of loading rate on a beam at room temperature and comparison of several welded beams at $-115°$ F are discussed later. As noted previously, only a limited number of "static" actually low straining rate tests were made because the results were inconclusive in differentiating the steels and treatments with respect to brittle behavior.

Impact Tests

The major part of the test program consisted of increment drop impact tests. The tower structure providing guides and lifting facilities for the tup was described in the report of previous impact tests. Some modifications were made in the beam supports and instrumentation, and the entire tower was re-erected on a more massive concrete foundation, bearing on rock.

The striker weight or tup weighing 2000 lb consisted of a block of steel to the lower end of which was attached a $4\frac{1}{2}$- x $4\frac{1}{2}$- x $15\frac{3}{4}$-in. contact block of alloy steel with bottom rounded to a 3 in. radius. The tower was 20 ft high, providing a net height of fall for the tup of 9 ft.

The cooling chamber was the same as that used for the static tests with an opening in the top panel to permit passage of the falling tup for centrally applied impact. This opening was normally closed with a movable cover, opened only when the blow was applied. Figure 8 shows details of the test assembly and Plate 2 shows the tower and cooling chamber enclosing a beam mounted for test.

The heavy steel pedestals on which the beam was supported were anchored to the foundation. The beam-supporting fixtures were intended to provide, as nearly as possible, unrestrained "simple" beam conditions and prevent rebound. The upward forces developed at the supports, corresponding to the reactions on the beam when deflected upward during the vibration cycle, were of considerable magnitude and during the earlier tests caused rupture of fixture and anchor bolts. The fixtures used permitted one end to rotate but prevented sliding, while at the other end permitted longitudinal movement as well as rotation. The clamping details for these fixtures are shown in Fig. 9. While these fixtures were effective in preventing upward rebound at the supports, the dynamic deflection records indicate rapid damping of vibration probably due to unavoidable friction in the support fixtures.

All beams were subjected to central impact by the 2000-lb tup in drop increments of 3 in. up to a fall of 36 in. and thereafter in increments of 6 in. To minimize the effect of local contact pressures at the point of impact and avoid application of the load directly to the weld, a 3- x 6- x 12-in. contact block was attached to the upper flange at midspan. The top of this block was machined before each test to present an undented surface. In the earlier tests this block was held in place by two inverted angles welded transversely to the upper flange. The block was grooved to avoid bearing on the weld and the angles

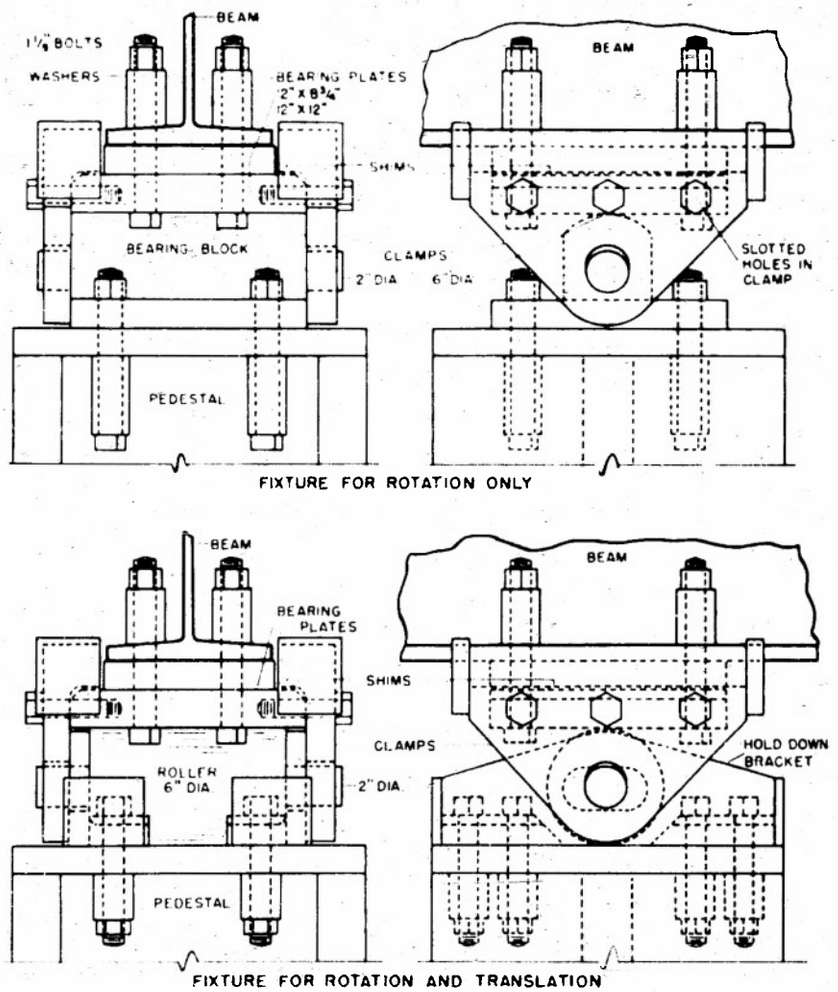

Fig. 9 Beam supporting fixtures for impact tests

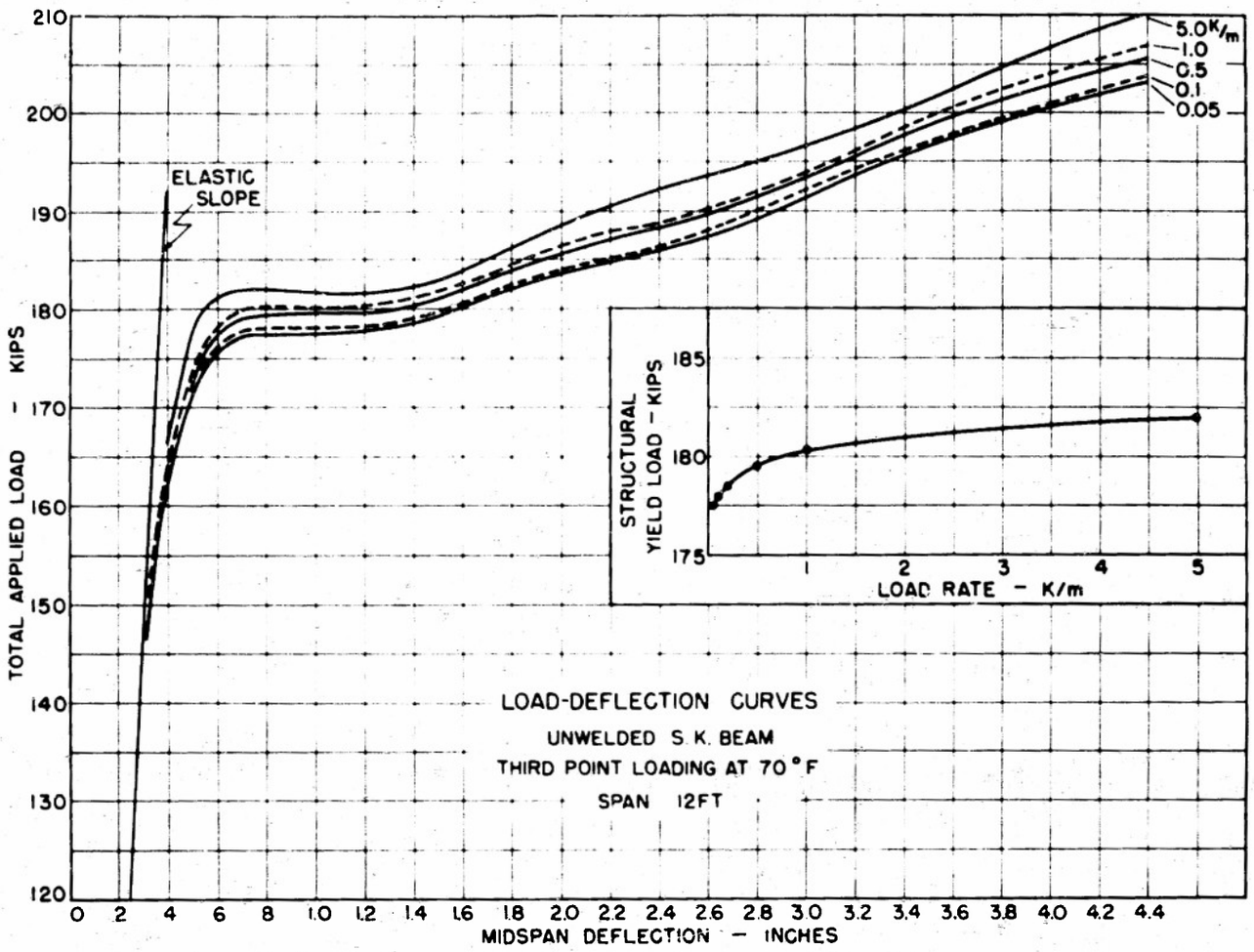

Fig. 10 Effect of rate of loading derived from relaxation of load at constant deflection

effectively held the block in place. Due to the flexibility of the angle legs, there was no appreciable flexure participation of the block with the beam section. Some of the complete fractures at low temperatures, starting at the lower flange extended through the upper flange adjacent to the bearing block close to the welds attaching the angles. Due to the possible influence of these angle welds in determining the location of the top flange fracture, the method of holding the contact block was changed to a simple bolted connection. Four bolts directly connected the block to the flange. While some fractures also occurred near the ends of the block, held by this method, no fractures occurred through the bolt holes.

In all tests, the beam either fractured or developed lateral buckling of the top flange with resulting pronounced over-all distortion of the section. The first tests, made at −115° F were in the nature of pilot tests for comparison with the static tests made at the same temperature. Fractures resulted in beams of both steels and all treatments. Thereafter, tests were made at successively higher temperatures to determine the temperature above which the type of failure was due to normal beam buckling without cracks.

The midspan dynamic deflection was measured at all blows. The apparatus used for deflection measurement consisted essentially of an optical system in which a beam of light passing under the beam was directed to a photo-tube and partially intercepted by a cut-off plate attached to the beam. In order to extend the intercepting plate below the cooling chamber the plate was attached to the end of a rod welded to the bottom flange about 1½ in. away from the splice on the beam centerline. The system is similar to that described for earlier tests, with an improved amplifier. The dynamic deflections were recorded on film by an oscillograph. The accuracy of the measurements was about ±0.005 in.

Dynamic strain measurements were made by SR-4 gages placed on the upper curved surface of the edge of the lower hole in the web and at points adjacent to the hole in the web and flange. Additional gages on the web weld measured permanent sets with a manual strain recorder. The equipment for dynamic measurements included David Taylor Model Basin strain indicators and a Hathaway oscillograph, adapted to the requirements of these tests. Four channels were available, recording strain transients and calibrations on a film record.

Strains were measured on beams of all types during

the earlier impact tests. In addition to determining the range of elastic action for comparison with the deflection measurements, the records served to indicate the start of cracks. When the behavior pattern was established, these strain records were discontinued and the proportional limit or structural yield strength was determined by the deflections.

In order to determine the amount of plastic deformation produced at critical locations adjacent to the fractures, scratch measurements were recorded for many of the beams. Prior to test, fine scratches spaced 0.1 in. apart were made over a length of 3 in. along a longitudinal line on the web immediately above the lower hole and also on the lower flange surface across the weld. The displacement of these scratches gave some indication of the amount of plastic deformation preceding or associated with the fracturing process.

RESULTS OF STATIC TESTS

These pilot tests at a temperature of −115° F were intended to determine the advisability of further tests at varying temperatures. While the results did not differentiate the beams and treatments as regards the brittle fracture phenomena, they do afford some comparison of beam behavior of the two materials, the effect of loading rates and the effects of the web holes on the strains in the vicinity of the splice.

The effect of loading rate in these so-called "static" tests, which are really tests at low loading rates, is indicated by the curves shown in Fig. 10, derived from the relaxation of load at constant deflection. The range of loading rates from these data is not large and the spread of structural yield strengths amounts to about 2.5%. The increase of yield strength would be considerably greater for the higher loading rates possible with ordinary testing machines when the loads are applied by the usual continuous beam test procedures where deflection measurements are made "on the run." The relation between loading rate and the structural yield loads is shown by the insert curve of Fig. 10.

Comparative load-deflection curves derived from relaxation data are shown for several beams in Fig. 11. The as-welded beams, both SK and FK,* have low ap-

* Reference to semikilled and fully killed steel will hereafter be abbreviated by SK and FK, respectively

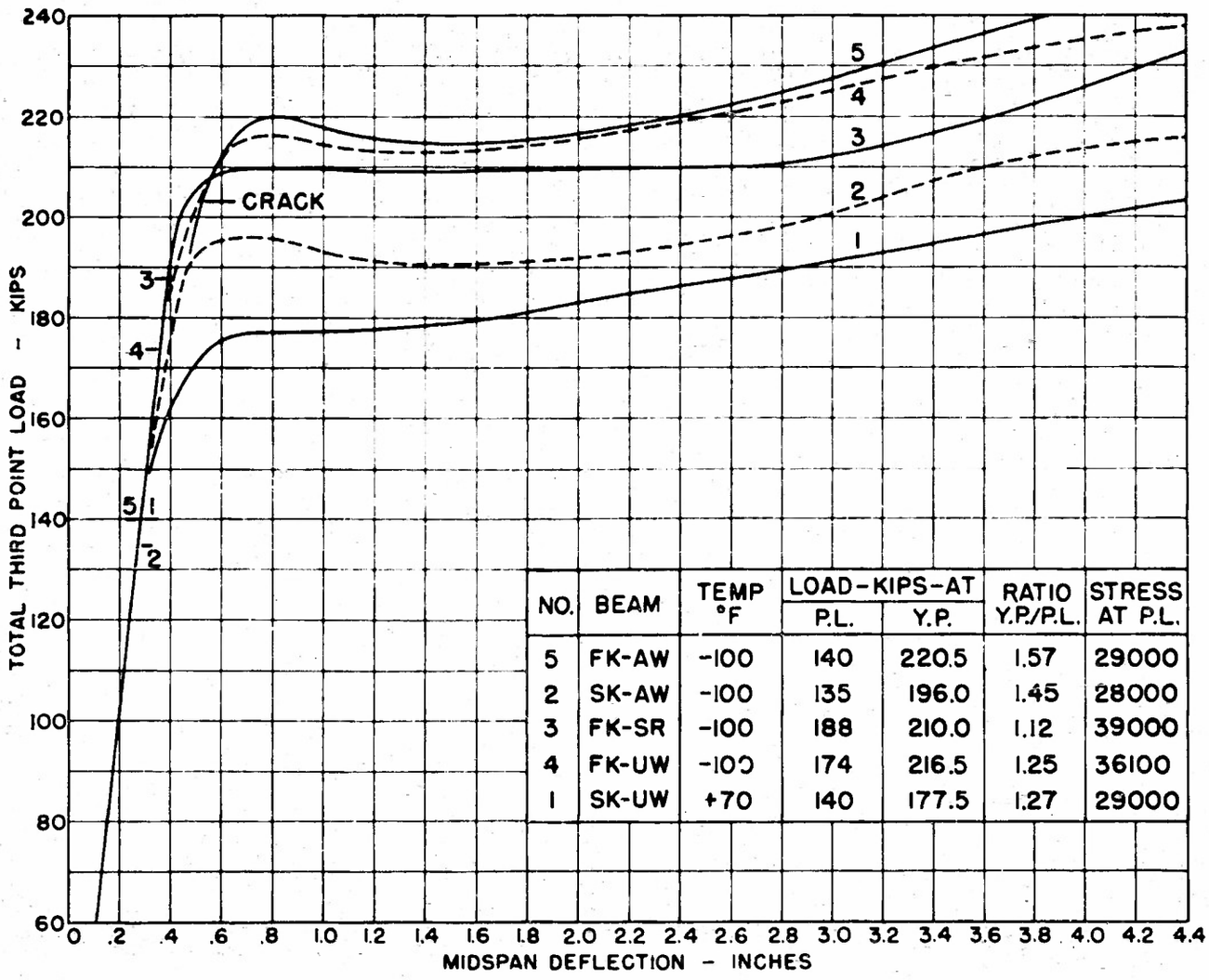

NO.	BEAM	TEMP °F	LOAD-KIPS-AT P.L.	LOAD-KIPS-AT Y.P.	RATIO Y.P./P.L.	STRESS AT P.L.
5	FK-AW	-100	140	220.5	1.57	29000
2	SK-AW	-100	135	196.0	1.45	28000
3	FK-SR	-100	188	210.0	1.12	39000
4	FK-UW	-100	174	216.5	1.25	36100
1	SK-UW	+70	140	177.5	1.27	29000

Fig. 11 Load-deflection curves at rate of loading of 0.05 kips/min

parent proportional limits due to residual stresses. The ratio of structural yield point to proportional limit is theoretically 1.15 for this section. The curves give values of 1.45 and 1.57 due to the lower PL. The FK, stress-relieved beam gave a ratio of 1.12 which is nearly the theoretical value indicating removal of residual stresses since the properties are not appreciably effected by this treatment. The unwelded FK beam at −100° F and SK beam at +70° F also showed somewhat high YP/PL ratios, probably due to rolling residuals. These limited tests give some indication of the beam properties, reflecting material properties and effect of temperature, although data are not available over a range of temperatures because this series of tests was discontinued.

All of the beams tested statically developed "refusal" loads by lateral buckling of the compression flange. One as-welded, FK beam tested at −100° F (Curve 5) cracked suddenly in the web at a deflection of 0.53 in. and at a load below the structural yield strength. This crack, starting at the end of the web weld at the top of the lower coped hole, extended to mid-height of the web (neutral axis). It did not extend beyond its initial formation with subsequent loading to buckling. Strain measurements indicated that appreciable permanent deformations in the web adjacent to the hole developed prior to the crack.

The partial fracture of the web with flanges remaining intact was found by later impact tests to represent an intermediate type of failure between buckling, with no cracks, and complete shattering of the entire section; that is, a tendency of crack propagation in the transition range. The formation of a brittle crack suggests therefore that the test temperature was in the brittle range. However, the unexpected fracture of a FK beam rather than a SK beam having less favorable properties, at the same temperature, is contrary to the findings of the impact tests and its significance is questioned. The relative tendency to brittle behavior was not established by these static tests.

Strain Analysis

Extended surveys of the strain distribution in the vicinity of the splice were made on the beams tested statically. The purpose of these strain surveys was to determine the influence of the holes in the web adjacent to the flanges, particularly in the plastic range. The findings are of particular interest as regards the origin of fractures produced in the impact tests.

The measurements extended over a length of 32 in. in the segment of constant bending moment between third-point loads. Longitudinal strains were measured with SR-4 electric gages placed on the flanges and web so as to determine the distribution over the beam section at the weld, 1¼ in. from the weld and at sections remote from the splice. Additional gages were placed to find the lateral distribution on the outer flange surfaces and the variation along the flanges.

The results obtained on beams of both materials were in substantial agreement with respect to the influence of the holes. The data presented represent the performance of a SK beam, as-welded, tested at −100°

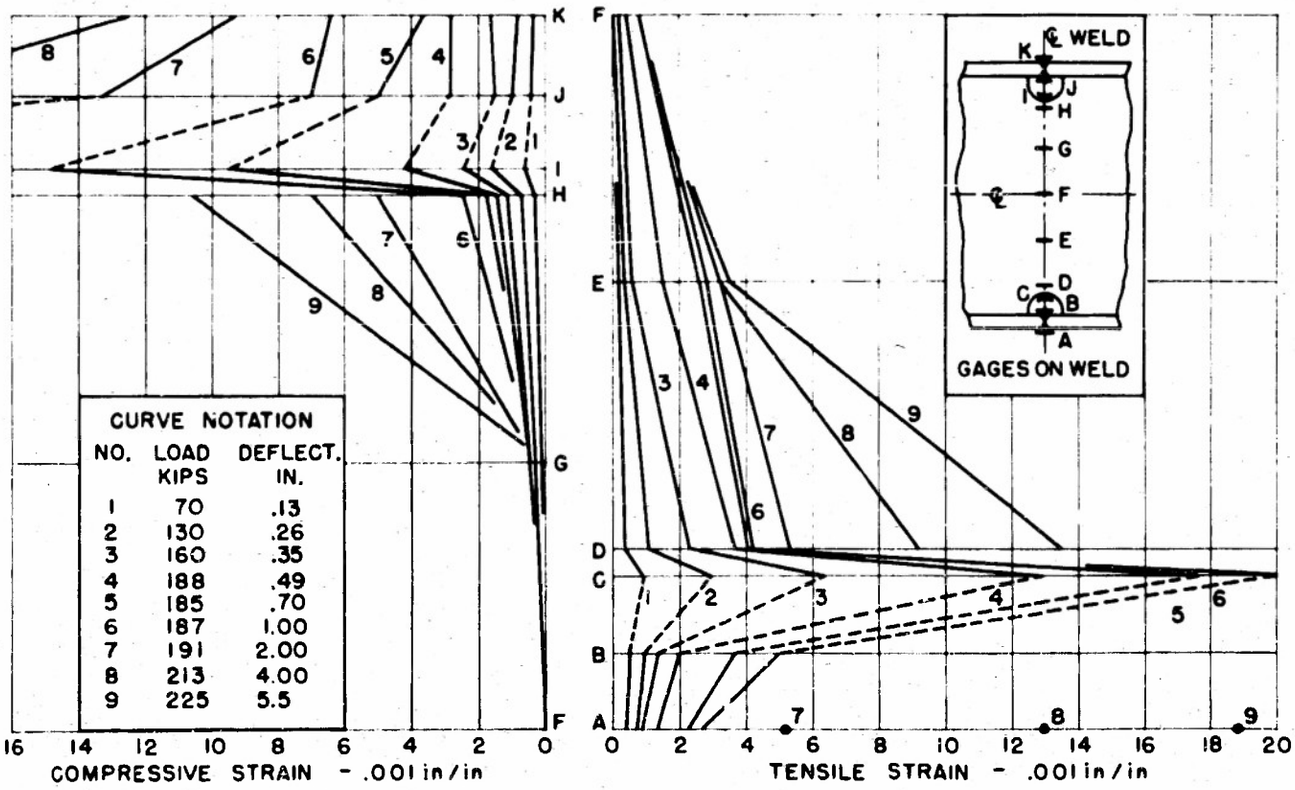

Fig. 12 Distribution of longitudinal strains on beam section

F. The distribution of longitudinal strains measured on the welded splice section, with weld reinforcement ground flat, is shown in Fig. 12. Gage stations *A* and *K* were on the tension and compression flange surfaces, respectively, directly opposite the web. Gages *B* and *J* were on the inner surfaces of the flanges, in the web hole. Gages *C* and *I* were on the curved edge of the hole, while *D* and *H* were on the web, $\frac{1}{4}$ in. from the edge of the hole. Gages *E*, *F* (centerline) and *G* were on the web surface. The curves plotted were for the deflection increments and total loads, applied at the third points of the span, as shown. Plotted values represent the average of two gages on opposite sides of the web and the average of two adjacent gages on the outer flange surfaces.

The influence of the holes in the web is indicated by the nonlinear distribution and the large concentrations of strain at the curved edges of the holes. This concentration is apparent in the elastic loading range with a factor of about 2 and increases rapidly with plastic deformation. The distribution is similar in both the tension and compression regions. Tension gages were lost at about 2.0% strain but, on the compression side, strains of 4.6% were measured at a beam deflection of 5.5 in. when the test was discontinued. The neutral axis moved toward the compression flange with large plastic deformations. A similar strain analysis was made at a section 8 in. from the weld splice where no hole existed. The distribution was found to be more nearly linear but with a tendency for the tensile strains at the level corresponding to the top of the hole, to lag under the large plastic deformations, probably reflecting the large strains developed at the neighboring section due to the hole.

The distribution of longitudinal strains along the centerlines of both flanges was measured over a distance extending 16 in. each side of the splice. Pairs of gages were placed on the weld, $1\frac{1}{4}$ in. from the weld and at more remote distances. The curves shown in Fig. 13 indicate the start of yielding and rapid increase of plastic strain in the base metal $1\frac{1}{4}$ in. from the center of the weld. The unsymmetrical appearance of these curves in the vicinity of the weld is due to the lack of corresponding measurements adjacent to, but on the other side of, the weld, where the curves are shown dotted. With increasing deformation there is a decided strain lag in the weld metal; that is, the weld metal is stiffer.

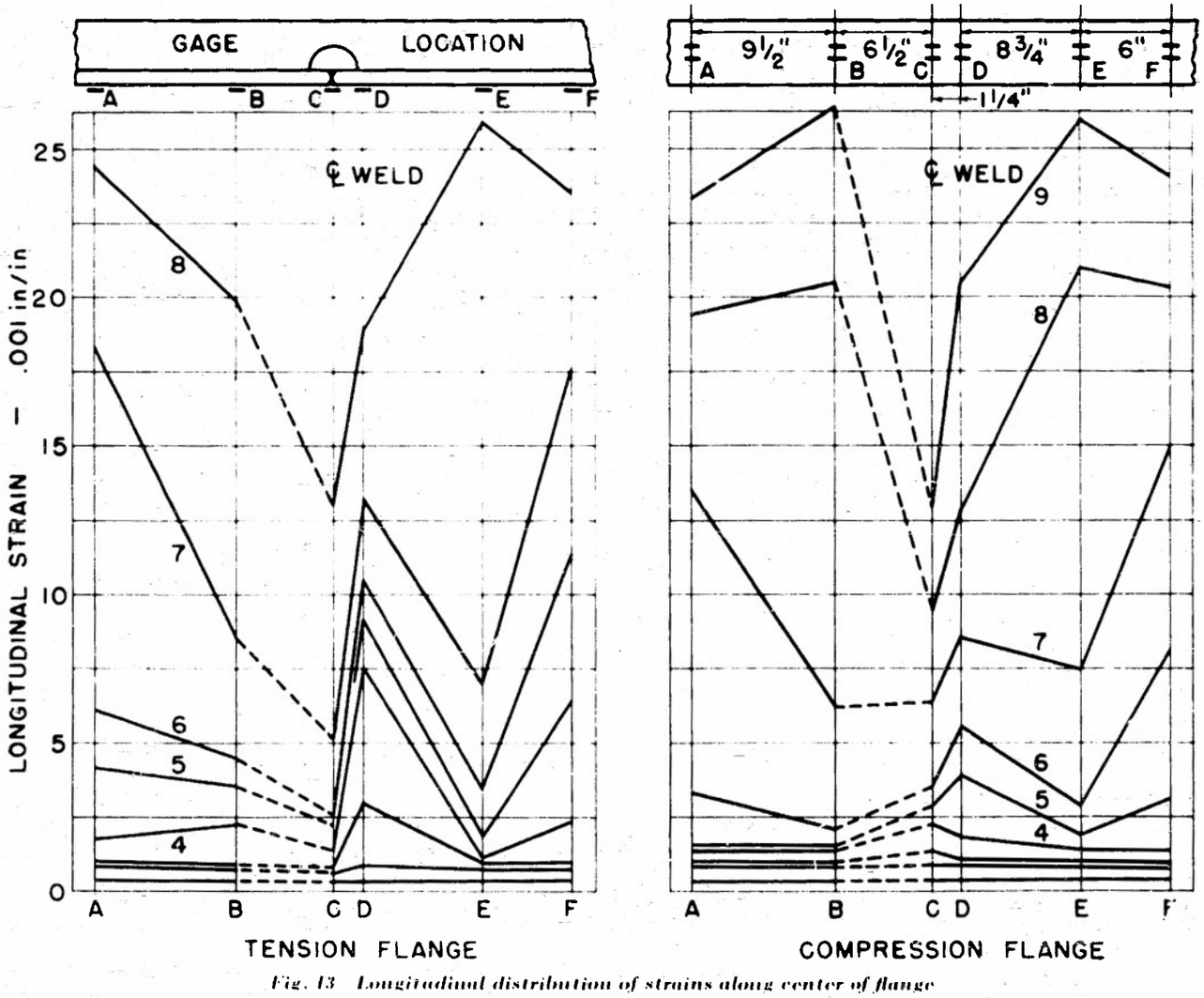

Fig. 13 Longitudinal distribution of strains along center of flange

The transverse distribution of strain on the flange surfaces is shown in Figs. 14 and 15. While the elastic strains are uniform across the flange, yielding progresses much more rapidly under the web. The pair of gages were opposite the web fillets and strains may have been larger on the centerline. The corresponding load curves indicate larger strains at the stations 1¼ in. from the weld. Yielding also progressed more rapidly under the web at a section 10 in. from the weld indicating normal behavior of the rolled section in which the strain at the edges of the flange tend to lag particularly on the tension flange. Buckling of the compression

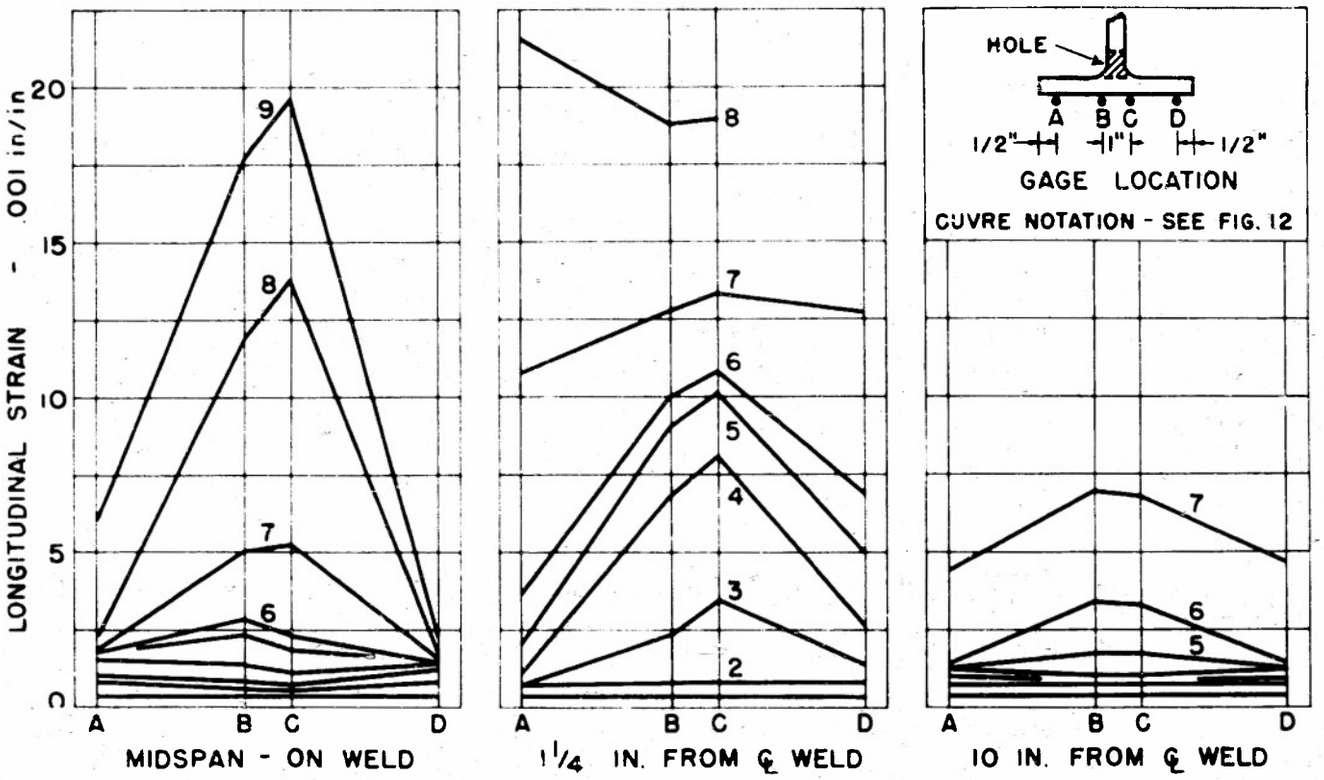

Fig. 14 Transverse distribution of longitudinal strains on tension flange

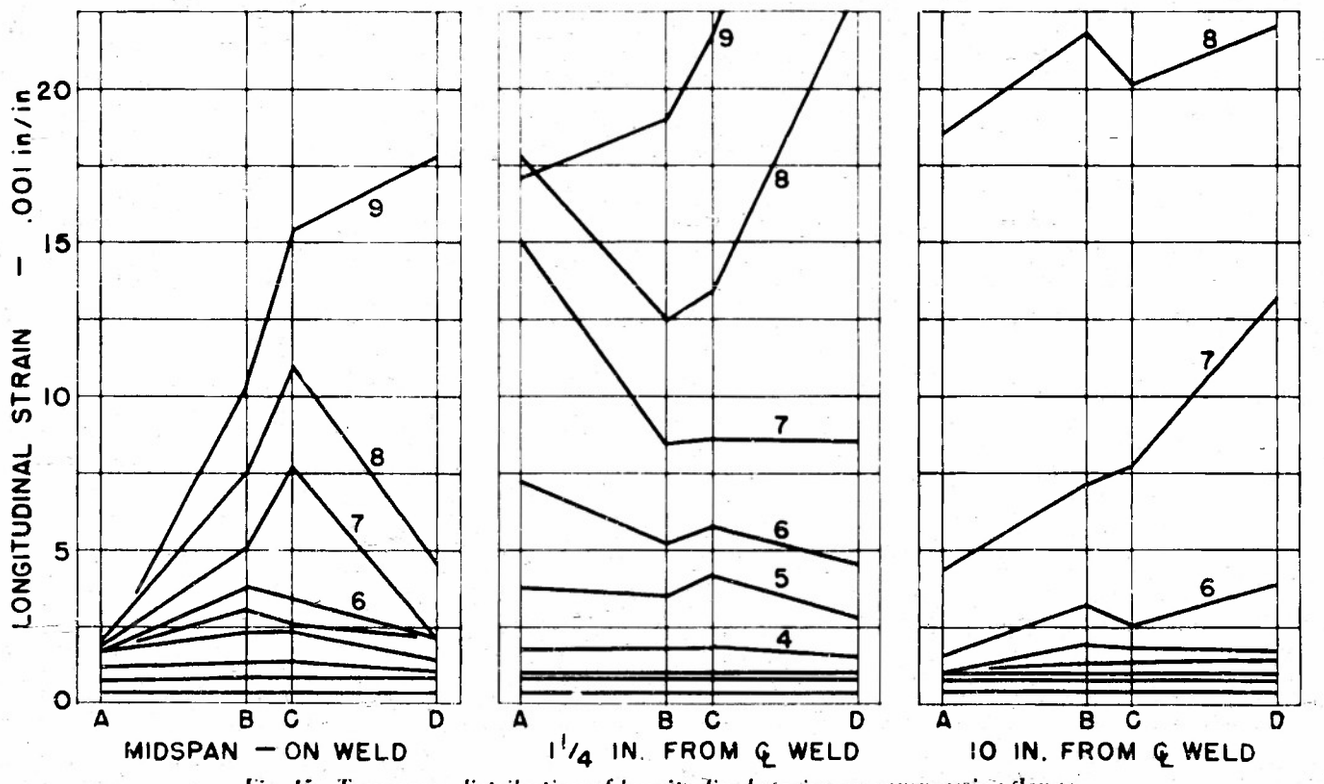

Fig. 15 Transverse distribution of longitudinal strains on compression flange

flange tends to increase the edge strains.

As will be discussed later, an estimate of the strain rate produced by dynamic loading of these beams is complicated by the wide variation of local strains. For a particular deflection rate, the strain rate would be greatest at points of greatest strain. The origin of fractures produced in the impact tests confirm the results of these strain analyses.

RESULTS OF IMPACT TESTS

The experimental data recorded in these tests of centrally applied impact by successively increasing drops of a 2000-lb tup included dynamic deflection and strains, independent dial gage measurements of permanent deflection set at each blow, permanent deformations by scratch displacement measurements after test and crack propagation observations. Most of the derived relationships were based on the deflection data. The strain records made on the earlier beams tested confirmed the elastic range found from the load-deflection relations and the initiation of cracks. These strain measurements were discontinued in the later tests. A summary of test results and derived data is given in Table 5 which includes supplementary tests to be discussed later. This summary includes the height of fall at which fracture was produced or the height when tests were discontinued because of pronounced distor-

Table 5—Results of Impact Tests on Butt-Welded Beams

Mark	*Temperature, °F*	*Height of fall, in.**	*Strain energy ft-kips,†*	*Deflection in.,‡*	*Equivalent loads, kips PL.*	*YP§*	*Ratio YP/PL.*	*Stresses, ksi PL.*	*YP*	*Failure*
Semikilled steel, as-welded, E6011-20 electrodes										
1E1	−114	60	7 2	0 55						Complete fracture
4C	−40	66-78	10 8-18 7	0 79-1 18	222	266 5	1 20	69 0	82 7	Web fracture to complete
4C1	−30	90-108	24 6-50 6	1 45-2 85	210	262	1 25	65 2	81 4	Web fracture to buckle
5C	−20	96-108	31 3-42 8	1 80-2 42	199 5	254	1 275	62 0	78 9	Web fracture to buckle
2D	−10	108	56 5	3 14	195	243	1 245	60 5	75 5	Buckled
1D1	−10	109	52 3	2 74	195	251	1 30	60 5	78 9	Buckled
4A	0	90	31 6	1 61	180	229	1 27	55 9	71 1	Web and lower flange fracture
1D	+5	84	27 3	1 72	175	232	1 325	54 3	72 0	Buckled
2E	+10	102	41 2	2 53	170	229	1 345	52 8	71 1	Buckled
4A1	+20	108	48 7	2 97	180	226 5	1 26	55 9	70 4	Buckled (small crack)
						Avg	1 275			
Semikilled steel, welded and stress-relieved E6011-20 electrodes										
5E1	−148	60	7 6	0 60						Complete fracture
3E1	−40	72	12 7	0 92	235	258	1 10	73 0	80 1	Web and lower flange fracture
2D1	−25	78	19 0	1 17	213	253	1 19	66 1	78 5	Complete fracture
4B1	−15	60	8 8	0 63	225	250	1 11	70	77 6	Web and lower flange fracture
3D	−10	102	32 4	1 94	200	249 5	1 245	62 1	77 5	Buckled
4B	−5	60-72	8 5-17 3	0 70-0 94	204 5	242	1 182	63 5	75 2	Web fracture to complete
5A	0	78-84	20 6-23 8	1 32-1 48	205	243	1 185	63 6	75 5	Web and lower flange fracture
5B1	+5	96	29 8	1 84	196	241	1 23	60 9	74 9	Buckled
3D1	+15	90	29 0	1 79	185	236	1 275	57 4	73 3	Buckled
5E	+30	110	53 6	3 63	180	215	1 19	55 9	66 8	Buckled
						Avg	1 19			
Semikilled steel, preheat and welded, E6011-20 electrodes										
3E	−115	33	1 1	0 47	...	...	...	...	...	Complete fracture
4D	−40	72	13 4	0 92	210	...	...	65 2	...	Web and lower flange fracture All outside weld zone
3A	−39	107	13 1	2 20	220	270	1 23	68 1	83 8	Complete fracture
2E1	−25	54-66	8 1-11 5	0 69-1 11	208	244	1 17	64 6	75 7	Web and lower flange fracture
4D1	−20	30	3 8	0 47	...	...	...	...	...	Lower flange only fracture
5D1	−15	108	40 6	2 33	195	248	1 27	60 5	77 0	Buckled
5A1	−10	108	13 2	2 49	195	246	1 26	60 5	76 4	Buckled
5D	−5	90	27 1	1 69	190	234 5	1 24	59 0	72 8	Buckled
						Avg	1 23			
Fully killed steel, as-welded, E6011-20 electrodes										
8A	−120	84	14 6	0 90	209	295	1 41	64 9	91 6	Complete fracture
4D1	−60	48-60	6 4-9 4	0 59-0 75	212	...	...	65 8	...	Web fracture to complete
6D	−50	84-90	21 6-34 6	1 33-1 96	220	252 5	1 15	68 3	78 4	Web and lower flange fracture
1B1	−50	108	36 0	1 70	220	259 5	1 18	68 3	80 5	Buckled
7E	−40	96-108	39 0-46 3	2 21-2 63	179	250 5	1 40	55 6	77 8	Web fracture only
6D1	−35	60-78	9 5-17 0	75-1 16	217	...	...	67 4	...	Web fracture to complete
8A1	−32	96-102	35 0-40 3	2 07-2 36	195	240	1 23	60 5	74 5	Web fracture only
4D	−26	90	24 7	1 50	207	247	1 19	64 3	76 7	Buckled
8E1	−20	102	41 6	2 50	170	239 5	1 41	52 8	74 4	Buckled
1B	−10	84	22 6	1 47	179	231 0	1 31	55 6	72 6	Buckled
						Avg	1 29			

tions caused by buckling. Where two values of height of fall, deflection and strain energy are shown, the first represents the blow producing first crack and the second represents a major extension of this crack in either the flange or web, or the value at which the test was discontinued due to buckling of the beam. The maximum height of fall available was 108 to 110 in.

Equivalent Static Loads

The vibration and subimpact phenomena of centrally applied impact was discussed in a previous report.[1] The elastic dynamic deflection can be predicted very closely by the approximate formula for the equivalent static load producing the same center deflection, with

Table 5—Results of Impact Tests on Butt-Welded Beams (*Continued*)

Mark	*Temperature, °F*	*Height of fall, in.**	*Strain energy, ft-kips,†*	*Deflection in.,‡*	*Equivalent loads, kips* PL	VP§	*Ratio,* VP/PL	*Stresses, ksi* PL	VP	*Failure*
				Fully killed steel, welded and stress relieved, E6011-20 electrodes						
7E1	−117	72-78	9.8-11.5	0.72-1.06	312			96.9		Web and lower flange fracture
5A	60	96-108	30.2-47.0	1.60-2.27	255	276	1.08	79.2	85.7	Web and lower flange fracture
2B1	55	15	1.9	0.32						Web and lower flange fracture
4E1	50	54-96	9.1-43.1	0.71-2.38	240	279	1.16	74.5	86.6	Web and lower flange fracture
5A1	−10	96	33.2	1.76	230	250	1.09	71.4	77.6	Buckled
2B	−30	96	33.1	1.92	220	242	1.10	68.3	75.1	Buckled
1E	−20	96	39.6	2.16	215	243.5	1.13	66.8	75.6	Buckled
						Avg	1.14			
				Fully killed steel, preheat and welded, E6011-20 electrodes						
8E	−103	18	2.3	0.35						Complete fracture
6A1	−80	96	22.6	1.20	240	278.5	1.16	74.5	86.5	Complete fracture
6A	−70	54-72	6.8-14.8	0.60-1.02	236	245	1.04	73.3	76.1	Web and lower flange fracture
5B1	−65	36	4.3	0.49						Web and lower flange fracture
5E	−60	108	24.0	1.38	225	275	1.21	69.9	85.4	Buckled
5B	−55	51	7.2	0.63						Complete fracture
3B1	−50	96	27.1	1.60	209	255	1.22	64.9	79.1	Buckled
3B	−40	102	32.2	1.88	200	252	1.26	62.1	78.2	Buckled
						Avg	1.18			
				Semikilled steel, unwelded, flame-cut holes in web						
2C	−115	48	5.7	0.56						Complete fracture
3C1	−60	108	31.05	1.81	200	276.5	1.38	62.1	85.9	Buckled
1C1	−40	96	27.3	1.61	190	259.5	1.37	59.0	80.5	Buckled
1C	−20	90	27.8	1.66	185	246.5	1.33	57.4	76.5	Buckled
						Avg	1.36			
				Fully killed steel, unwelded, flame-cut holes in web						
4B	−115	107	23.2	1.20	200	307	1.53	62.1	95.4	Complete fracture
6B	−60	81	20.1	1.42	185	254	1.37	57.1	78.9	Lower flange only fractured
8B1	10	66	13.0	0.81	160	254.5	1.59	49.6	79.0	Lower flange only fractured
6B1	20	90	21.7	1.44	110	233	1.66	13.5	72.4	Buckled
						Avg	1.54			
				Semikilled steel, unwelded, as stress relieved, drilled holes						
4E	−115	107			305	325	1.07	94.6	101.0	Buckled
				Semikilled steel, unwelded, drilled holes, pressed notch						
2C1	−60	48	6.1	0.60	225	...	...	70.0	...	Web crack at notch Lip = 0 to trace
3B1	30	42	5.3	0.53	215	...	...	66.7	...	Web crack at notch Lip = 0.01 in.
3B	+30	42	6.2	0.60	165	...	...	51.2	...	Web crack at notch Lip = 0.02 in.
				Fully killed steel, unwelded, drilled holes, pressed notch						
2D1	30	54	7.5	0.69	200			62.1	...	Crack at 54-in. drop, discontinued Lip = 0.015 in.
3D	+30	48-84	7.6-26.7	0.66-1.75	168	221.5	1.32	52.2	68.8	Crack at 48-in. drop Buckled at 84-in. drop
2D	+63	54-84	11.7-32.4	0.91	163	208.5	1.28	50.6	64.8	Crack started at 54-in. drop Buckled at 84-in. drop Lip = 0.10 in. (tear)

* Height of fall producing first crack or when discontinued due to buckle. Second value is height of additional increments to subsequent extended fracture or buckle as indicated.

† Total strain energy accumulated to first crack. Second value represents energy to subsequent buckle or extended fracture.

‡ Total deflection to first crack, subsequent buckle or fracture extension.

§ Equivalent static load producing elastic component of observed dynamic deflection.

Computed by flexure formula.

the appropriate inertia correction factor.* The elastic deflection predicted from this equivalent static load agreed with actual dynamic observations within less than 2%. It was also found that the observed dynamic deflections, prior to buckling of the beam, varied linearly with the striking velocity of the tup, as predicted by the equivalent static load formula, where P_{eq} is proportional to $V\sqrt{h}$. The primary assumptions made in deriving this approximate formula are (1) that the contact losses are negligible and (2) that the elastic deflection curves at maximum deflection are the same when loaded statically or dynamically. That the elastic curves are practically the same was shown by measurements of deflection along the beam as previously reported.[1] The relatively small indentations produced in the bearing block struck by the tup and the rigidity of the supports justifies the assumption of small energy losses, prior to buckling.

In the plastic range, the equivalent static load was found from the elastic component of the dynamic deflection which was represented by the deflection recovery after the blow. Curves representing the equivalent static load plotted against the total deflection, including the dynamic deflection produced by the blow and the previous permanent set, were similar to the familiar static load-deflection curves as shown in Figs. 10 and 11. From these curves, the loads corresponding to the flexural proportional limit and the structural yield point (knee of curve) were determined and the corresponding stresses computed by the flexure formula. The proportional limit stresses thus found agree very closely with the indicated start of yield as measured by electrical strain gages.

* $P_{eq} = \sqrt{\frac{96\,EI}{L^3}\,\frac{W_b}{W_t}} \times C = 36.2\,C \times h^{\frac{1}{2}}$ approximately where C = inertia correction $= \frac{1 + \frac{17}{35}\frac{W_b}{W_t}}{\left(1 + \frac{5}{8}\frac{W_b}{W_t}\right)^2} = 0.72$ for W_b = weight of beam (1000 lbs.), W_t = weight of tup (2000 lbs.)

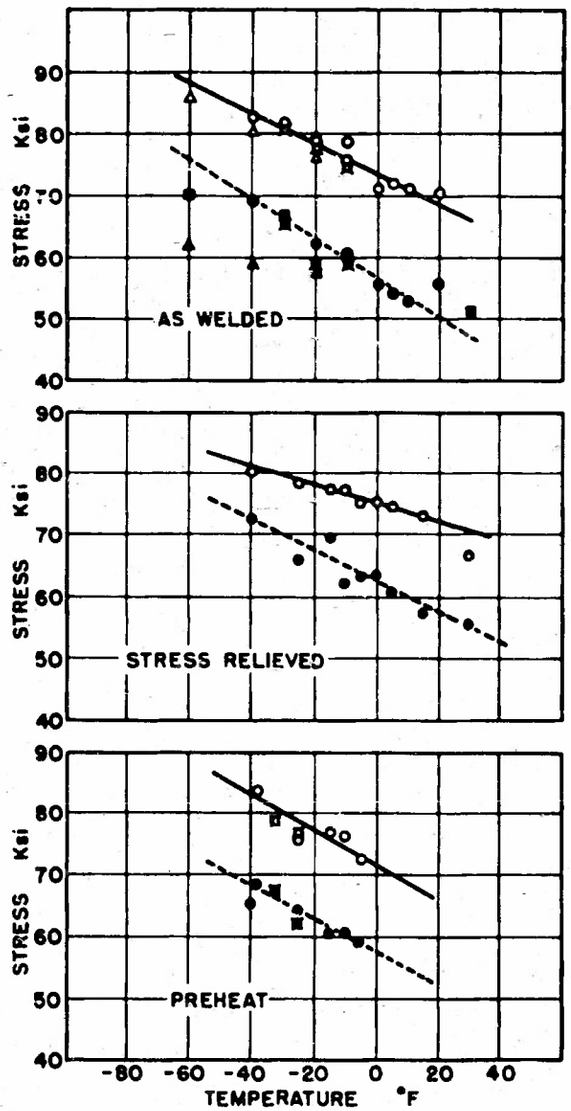

DYNAMIC FLANGE STRESSES — SEMI-KILLED STEEL

--- PROPORTIONAL LIMIT, —— STRUCTURAL YIELD POINT

WELDED ● ○ E 6010 ELECTRODES
✕ ✕ E 6016 ELECTRODES

UNWELDED ▲ △ FLAME CUT COPES
■ □ DRILLED COPE—PRESSED NOTCH

Figure 16

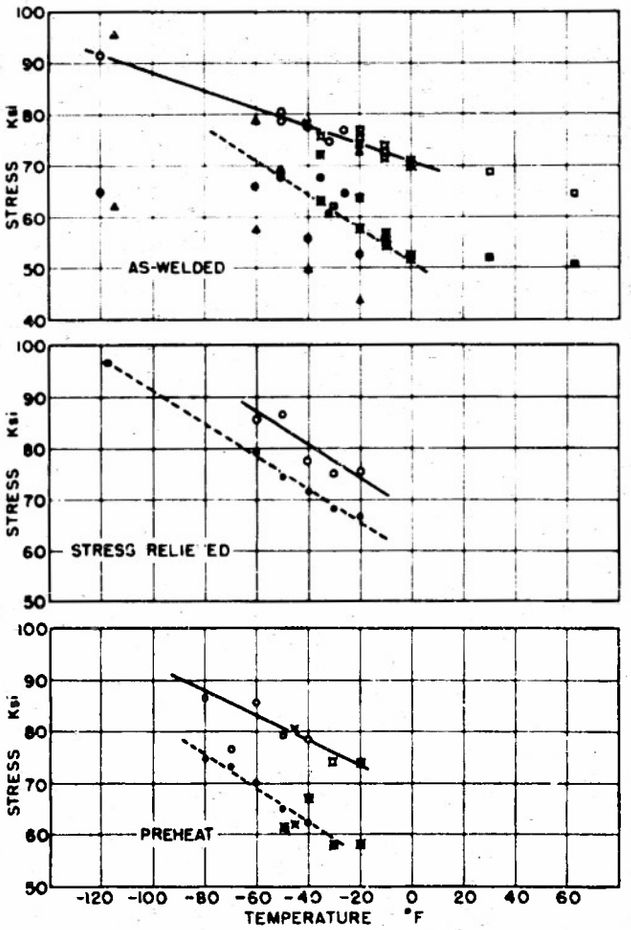

DYNAMIC FLANGE STRESSES — FULLY KILLED STEEL

----- PROPORTIONAL LIMIT, —— STRUCTURAL YIELD POINT

WELDED ● ○ E 6010 ELECTRODES
✕ ✕ E 6016 ELECTRODES

UNWELDED ▲ △ FLAME CUT COPES
■ □ DRILLED COPE—PRESSED NOTCH

Figure 17

The dynamic flange stresses for both steels and each of the welding treatments, and their relation to the test temperature, are shown in Figs. 16 and 17. The variations of stress with temperature are shown as straight lines over the range of test temperatures although flat curves might be expected. Both the proportional limit and yield point stresses increase with decrease of temperature. The higher values as compared with the tensile properties of the base metal are due to both temperature and rate of loading. The ratio of the structural yield point to the proportional limit is given in Table 5. The theoretical ratio for this beam section is 1.15. It will be noted that the as-welded beams of both steels show ratios of about 1.28 due to the lowering of the apparent proportional limit by residual welding stresses. When stress relieved, the ratios were 1.19 and 1.14 for the SK and FK beams, respectively, which agrees substantially with the theoretical value of 1.15, indicating that the residual stresses were effectively relieved. The preheated beams show somewhat less residual stress effect by those ratios than the as-welded beams.

Although tests were made on all types of beams at -110 to $-120°$ F, stress values are lacking in most of these diagrams because failure occurred by shattering fracture without developing any permanent deflection set; i.e., below the proportional limit. The elastic behavior of the beams fabricated with low-hydrogen electrodes is essentially the same as those welded with E6020 electrodes.

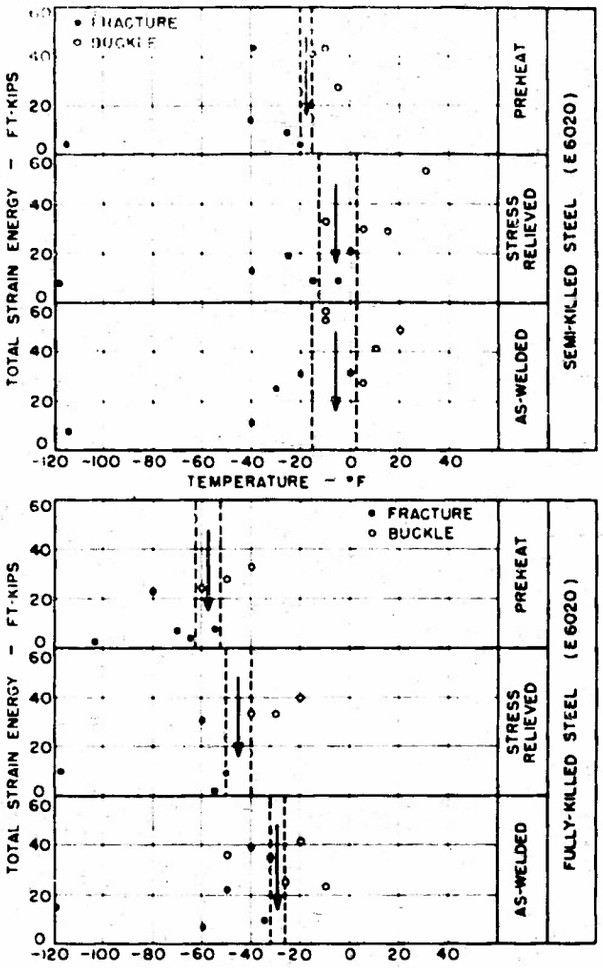

Fig. 18 Fracture-buckle transition temperatures

Strain Energy

The strain energy stored in the beam by the dynamic load is derived from the kinetic energy of the tup. However, part of the energy of the falling weight is expended in accelerating the beam so that theoretically the flexural strain energy represents 72% of the energy of the striking weight, for the weights of beam and tup used in these tests. This is the inertia correction factor included in the equivalent load formula. Additional energy losses are involved. Although contact losses can be neglected, a very considerable decrease in the energy available for flexure of the beam in the plane of loading may result when buckling of the beam develops because of the lateral deflection and twisting produced and the energy transmitted to the guides when the tup is deflected laterally by the distorted beam. The flexural strain energy may then represent only 50 to 60% of the kinetic energy of the tup.

The flexural strain energy was computed from the area under the equivalent static load-deflection curves, which are based on the observed dynamic deflections and permanent sets; that is, the actual beam performance. These strain energy values at first crack or buckle are shown in Table 5. The strain energy values to fracture or buckle for beams of both steels and each of the treatments when welded with E6020 electrodes, at the test temperatures are shown in Fig. 18.

The accumulated strain energy stored in the beam under successive blows as computed may be affected by strain aging. However, for the beams tested at temperatures below the transition range, the plastic deformations at fracture were small and because of the low temperature and short time intervals between blows, this possible aging effect is believed to be unimportant for the comparisons made here. Also, at the higher temperatures when buckling with considerable plastic deformation was involved, the exact energy value is not significant because the total energy is largely dependent upon the progress of buckling and when the test was discontinued.

In general, when fractures develop, the energy values are low. When buckling determines the ultimate behavior, the strain energy is considerably larger. Had the beams been braced laterally, much greater deflections could have developed with corresponding increase of plastic energy and the energy values would have shown a more abrupt drop in the fracture range. The points in Fig. 18 representing strain energy for beams in which the test was discontinued due to excessive buckling—namely, at the higher temperatures—are erratic and too low. Using the beam deflections rather than strain energy would not greatly change the comparison of behavior since both the deflection and

strain energy reflect the amount of plastic deformation developed.

Transition Temperatures

Figure 18 shows the temperatures at which a transition in type of failure from buckling to fracture occurs. This temperature is taken as the mean of a range of uncertainty within which there is a probability of either type of failure, according to the number of tests made. Based on this buckle vs. fracture criterion, transition temperatures are fairly well defined, as shown in Table 6.

Table 6—Transition Temperatures, ° F, for Butt-Welded Beams, Buckle vs. Fracture Criterion

Weld treatment, E6011 20 electrodes	*Type of steel*	
	Fully killed	*Semikilled*
As-welded	−29	−5
Welded-stress relieved	−45	−5
Welded with preheat	−57	−17

The results show lower transition temperatures for the welded fully killed steel beams by 24° F in the as-welded condition and 40° F for both the stress relieved and preheat treatments. While both steels show more favorable transition temperatures when welded with preheat, the effect is less marked in the case of the semi-killed steel, which also shows no improvement by stress-relieving treatment.

The two grades of steel selected for these tests had appreciable differences in low-temperature notch sensitivity. In both the Charpy and Kahn tests the FK steel showed lower base metal transition temperatures. The beam weldments also show more favorable transition temperatures for the FK steel and therefore seem to reflect, qualitatively, the base metal properties. More correctly, it is probable that both the notch sensitivity and weldability as indicated by the performance of the weldments, reflect the same inherent property that determines transition temperature and crack propagation. The variation of transition temperatures determined by the Charpy and beam tests, due to specimen location, arbitrary criteria and welding treatments, does not permit a quantitative correlation. The relation of Charpy values to crack propagation will be discussed later.

FRACTURES

The origin of the fractures was influenced by the weld and the geometry of the specimen; that is, the presence of holes in the web. The configuration of the fracture was also influenced to some degree by the method of loading. It has been shown that a large strain concentration was produced in the web at the inner edges of the holes. Likewise, the strains in the flanges were greatest adjacent to the weld, opposite the edges of the web holes. The strain rates under dynamic loads were also greatest at these points. The holes were formed by manual flame cutting. There were some gouge marks from the oxy-acetylene cutting on all specimens. The location of these holes immediately adjacent to the flange made it difficult to shape the holes and cut a flat flange surface because the torch had to be held so close to the flange. Before testing, the top edge of the hole and the surface on the flange on the tension side of all beams were smoothed with a file. This filing was done on the earlier beams tested to permit placement of electric strain gages on the inside curved surface and on the flat surface of the flange in the hole. Usually, this filing removed only the scalloped irregularities of flame cutting. Deep grooves could not be removed, particularly in the corners of the semicircular hole. This practice was continued when gages were not used, to maintain uniformity of conditions. While the gouging grooves are strain raisers, the root radii are relatively large and it was found that fractures frequently originated at other locations with smooth surfaces in spite of the existence of grooves which might be expected to invite the start of cracks. The surface irregularities themselves were probably not critical to the relative behavior of the beams. However, the formation of shallow thermal cracks and the modified structure at the flame-cut edges may have influenced the origin of fracture. Supplementary tests on unwelded beams with flame-pierced holes were made and are discussed later.

The beams were first tested at −110 to −120° F, at which temperatures complete fractures were produced. Tests were then made at increasing temperatures until failure resulted by buckling without fracture. In order to locate the transition temperature with a minimum of specimens, the tests were concentrated around the transition range. The extent and configuration of the fractures were related to the testing temperature, propagating further across the section and at lower deflections as the temperature decreased.

At the higher temperatures above the transition range, the beams buckled by sidewise deflection of the unbraced upper flange and twisting of the section. Very little local crippling of the web resulted under the loading block although in a previous investigation where beams were tested at room temperature, pronounced dishing of the web and local depression of the loaded flange was produced. The buckling of the beam as a whole without pronounced local distortions may be due to the heavier tup used in these tests. The maximum vertical deflection produced depended on the progress of buckling which determined when the test was discontinued. The large distortions demonstrated the lack of brittleness at these higher temperatures.

A photographic record was made of all beam fractures. The views shown in Plates 3 to 15 are intended to illustrate typical fractures in a sequence of propagation without regard to the particular steel or treatment but are identified for reference. A complete record of the type of fracture is given in Table 5.

The first visible sign of distress in the splice as the test temperature decreased was the formation of a "dimple" i.e., pronounced contraction of thickness

Plate 3 SK beam 5 A1 welded with preheat, tested at −40 F, buckled with deflection of 2.49 in. Web weld directly over hole "dimpled" with large deformation, no cracks

in the web immediately above the hole on the tension side. This local deformation was in the weld metal but at a point of maximum strain concentration (see Plate 3). No crack developed and the beam resisted dynamic load to buckling. The first cracks produced occurred at the top edge of the lower hole. As shown in Plate 4, these cracks, actually tears, extended $\frac{1}{2}$ to $\frac{3}{4}$ in. in the weld metal and did not propagate with subsequent blows. Some of these partial web cracks also extended to mid-height of the web, Plate 5, in or adjacent to the weld-up to the neutral axis and then entered the base metal, sometimes terminating in a "dimple" or local contraction where the energy was evidently dissipated by plastic deformation. The web cracks tended to branch and sometimes extended to the upper flange fillets. From the scale patterns on the web surface, this branching crack seemed to be avoiding the local compression zone under the loading block. However, the branching occurred at different heights

Plate 4 SK beam 4 A1 tested as-welded at +20 F. Tear in weld at top of hole. Beam buckled with deflection of 2.97 in. with no propagation of crack

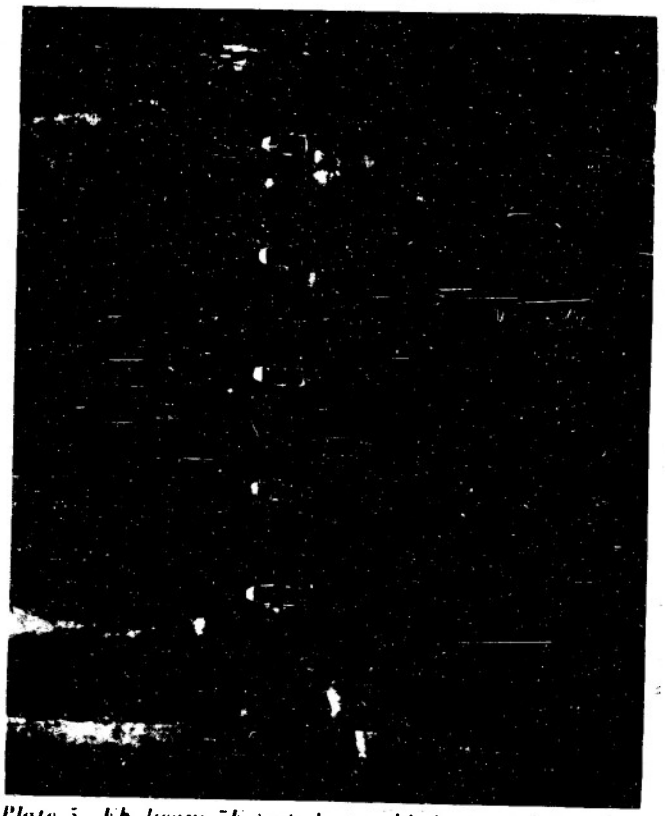

Plate 5 FK beam 7E tested as-welded at −40 F. Web crack started in weld at deflection of 2.21 in. and extended as shown at deflection of 2.63 in. Crack terminates in base metal with "dimple" at end

Plate 6 FK beam 6D tested as-welded at −50 F. Web crack started in weld at deflection of 1.33 in. Web crack extended and flange fractured at 1.96 in.

Plate 7 SK beam 3E1 stress relieved and tested at −40 F. Web and flange fractured at deflection of 0.92 in. Flange fracture about 1/4 in. outside weld

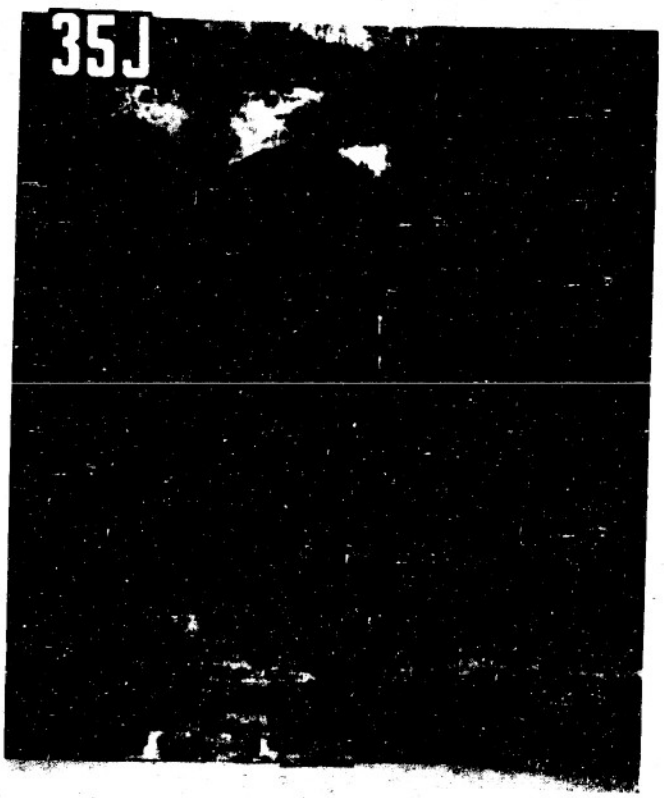

Plate 8 FK beam 6 A welded with preheat, tested at −79 F. Web crack started at hole at deflection of 0.60 in. Web crack extended with multiple web and flange cracks at 1.02 in.

of the web and in a few cases started close to the lower hole.

The next grouping of fracture patterns, as the temperature decreased, included fractures in both the web and lower flange. These combined fractures occurred simultaneously or in some cases the flange break occurred at a blow subsequent to that producing the web crack. Flange cracks occurred both in the weld metal and in the base metal at 1/4 to 3/4 in. from the edge of the weld. Two presumably unfavorable conditions exist at the latter location: namely, the heat-affected zone and the higher strains directly under the edge of the hole, with the possible additional effect of gouges due to flame cutting. Fractures of this type are shown in Plates 6, 7, and 8.

At the lower temperatures, considerably below the transition range, the fractures were complete, originating and propagating through the entire web and both flanges under the same blow. Typical fractures of this type are shown in Plate 9 to 12. The brittleness at these temperatures is indicated by the irregularity of the cracks and shattering tendency. The entire fracture occurred simultaneously, with small, elastic beam deflections and strain energy absorption.

Some exceptions to the general grouping of fractures are shown in Plates 13 to 15. Nothing unusual was observed to account for the fracture in the flange under the edge of the hole without a web crack. The fracture through the lower flange remote from the welded zone and propagating in the web without regard to the splice cannot be explained except that the beam was welded with preheat extending some distance either side of the splice which may have affected the material in some indeterminate manner. This is one of those unexpected results to which every investigation is entitled.

The fracture shown in Plate 15 is of interest because of the indicated origin of the crack at a weld not associated with the splice. In testing the beams early in the program, the loading block was held in place by inverted angles having the edge of one leg welded to the top surface of the flange with fillet welds (see Plates 11 and 12). The crack appeared to originate at a small spot on one of these welds and propagated through the base metal of both flanges and web. The fracture surface was fine grained, flat without chevron markings (temp., −124° F). It is interesting to note that while the upper flange is subjected to tension during the upward vibration cycle after the blow, the magnitude of the upward deflection during this first negative cycle is approximately only one-third of the downward deflection of the first forced vibration cycle, due to the rapid damping. Therefore the fracture originated in the upper flange weld attaching the angle at nominal stresses considerably less than those to which the butt splices were subjected and must be attributed to local imperfections in these particular welds since similar attachments on other beams behaved satisfactorily. The loading block was later held in place by simple bolted connections to avoid these additional welds. The

fracture does indicate the brittleness of the material at this low temperature.

The character of the fracture surface varied depending upon whether the break was within the weld or base metal. The fracture surface in weld metal was irregular and ragged, tending to become flatter at the lower temperature. Where the break occurred adjacent to the weld in the base metal, the fracture was coarse granular and often showed a chevron pattern pointing toward the top of the lower hole in the case of the web fractures or toward the bottom of the hole in the lower flange break. These lower flange fractures usually were more irregular toward the outer edges with the fracture becoming flatter with fine grain texture directly under the hole which is in the fillet region of the beam. In the case of branching web cracks wholly in the base metal (see photographs), the fracture surface usually was comparatively flat with fine granular texture although in some cases one branch would be granular while the other was ragged, changing to fine granular near the upper flange. The fracture in the upper flange was always fine granular. The appearance of the fracture is perhaps related to the speed of propagation which is changing with the reduction of beam section. In many of the branching web fractures progressing through the base metal a fine lip was found at the edges. Occasionally these lips were present in irregular, ragged breaks but were more distinct in the fine-grained frac-

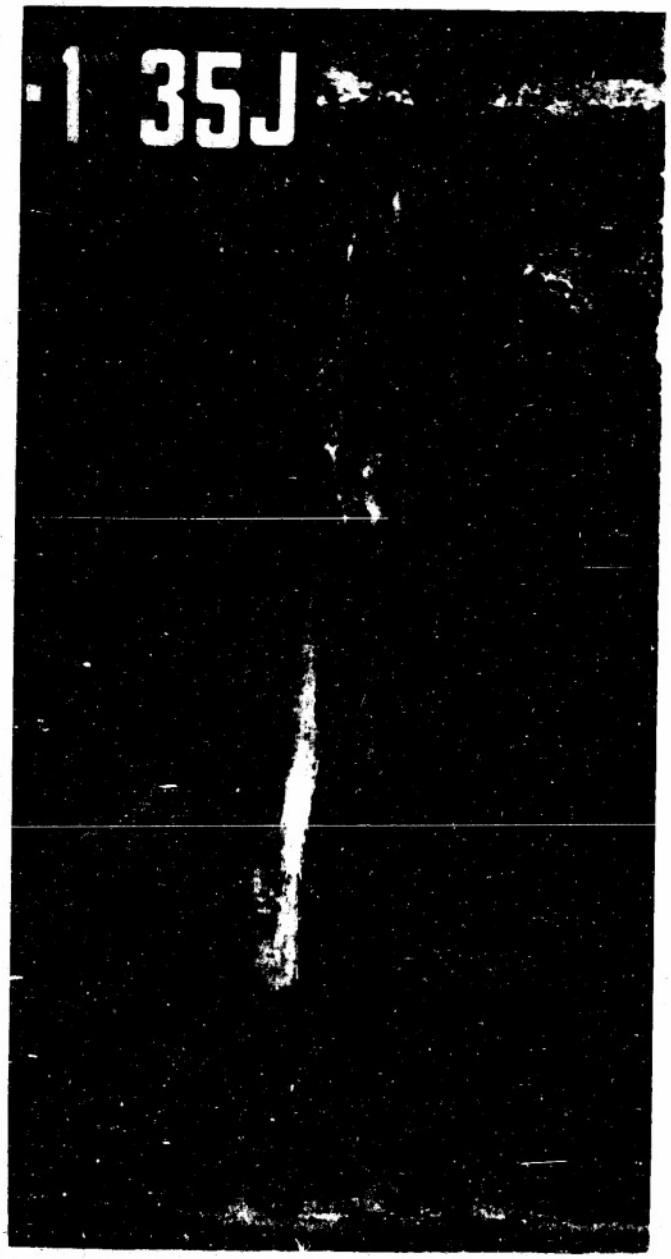

Plate 9 FK beam 6D1 tested as-welded at −35° F. Web crack started at deflection of 0.75 in., complete fracture at 1.16 in.

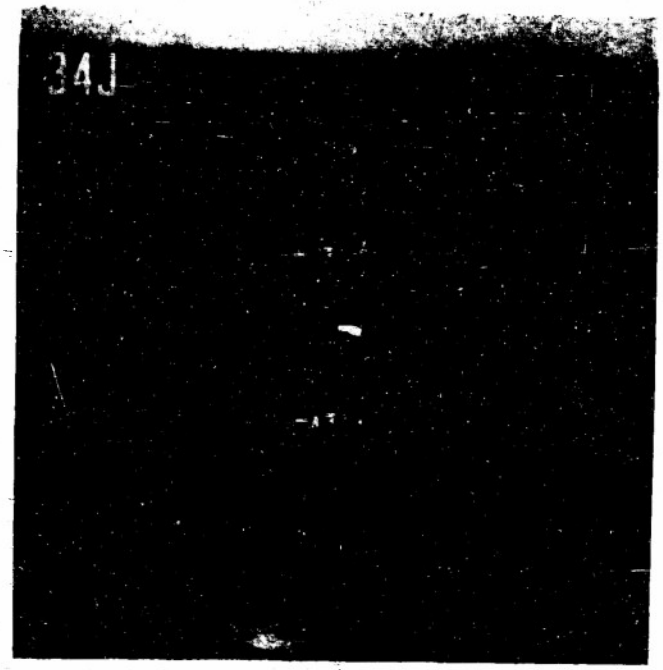

Plate 10 SK beam 5E1 stress relieved and tested at −118° F. Complete fracture at deflection of 0.60 in.

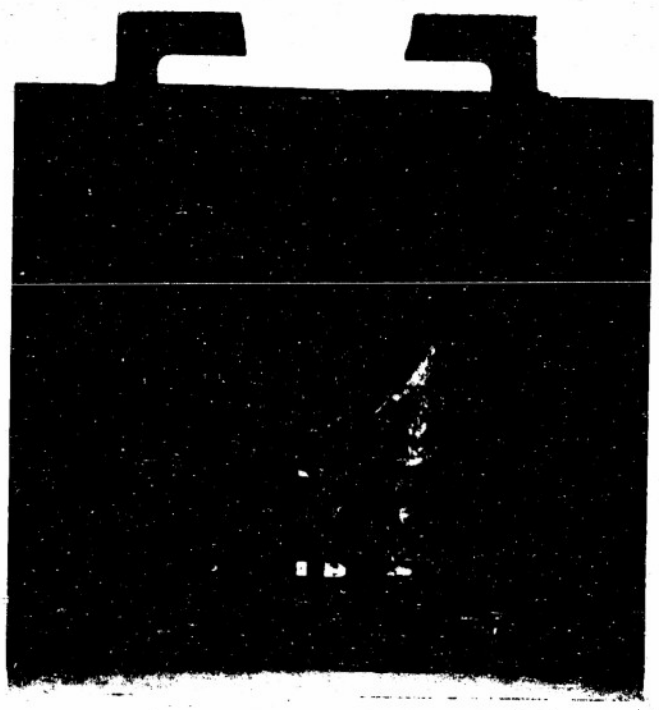

Plate 11. SK beam 3E welded with preheat, tested at −115° F. Complete fracture at deflection of 0.47 in. Early test using welded angles to hold loading block, fracture outside

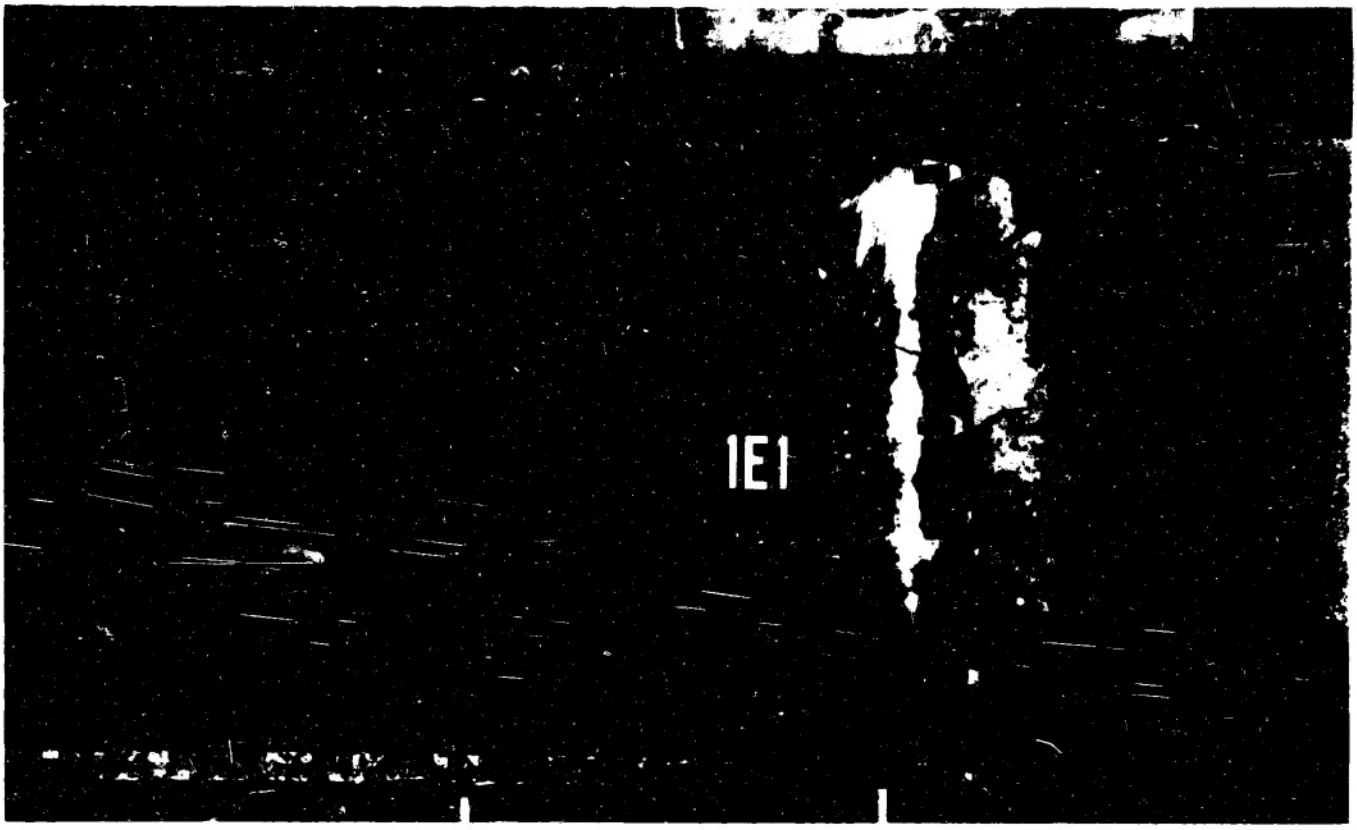

Plate 12 SK beam 1E1 tested as-welded at −114° F. Complete fracture at deflection of 0.55 in. Note irregular branching cracks and fine web crack to left terminating at lower flange fillet about 20 in. from the splice.

tures. No lips were found on the fractures produced at the extremely low temperature (−115° F) but were present at −60° F and higher. Additional observations concerning the formation of edge lips are given in the discussion of fractures produced when pressed notches were formed at the web hole to initiate a web crack in an unwelded beam.

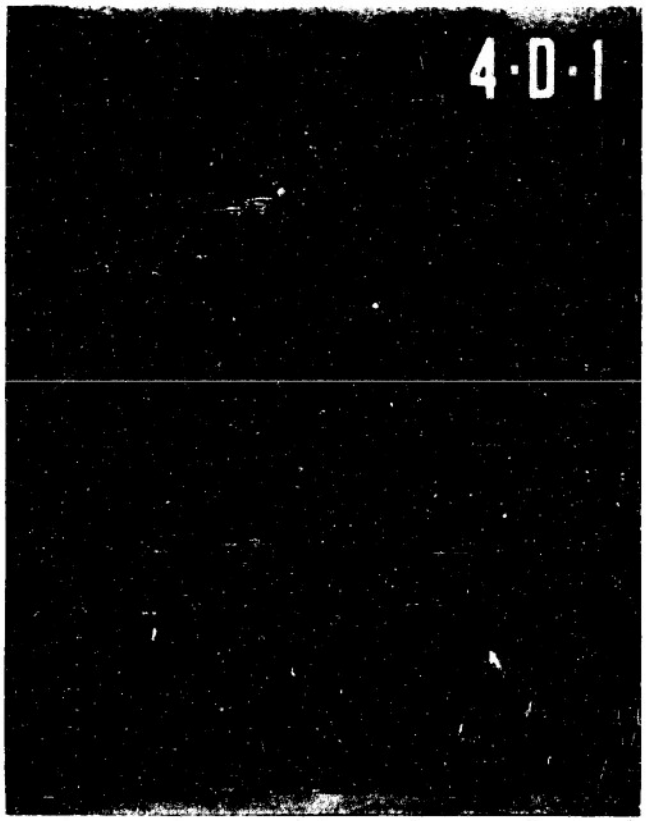

Plate 13 SK beam 4D1 welded with preheat, tested at −20° F. Fracture in flange only, outside of flange weld under edge of hole at deflection of 0.47 in.

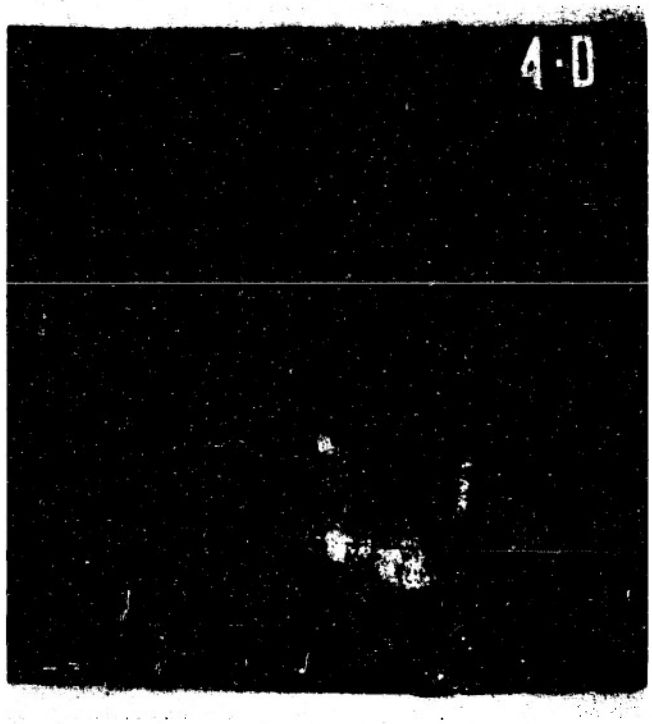

Plate 14 SK beam 4D welded with preheat, tested at −40° F. Fracture remote from welding zone at deflection of 0.92 in.

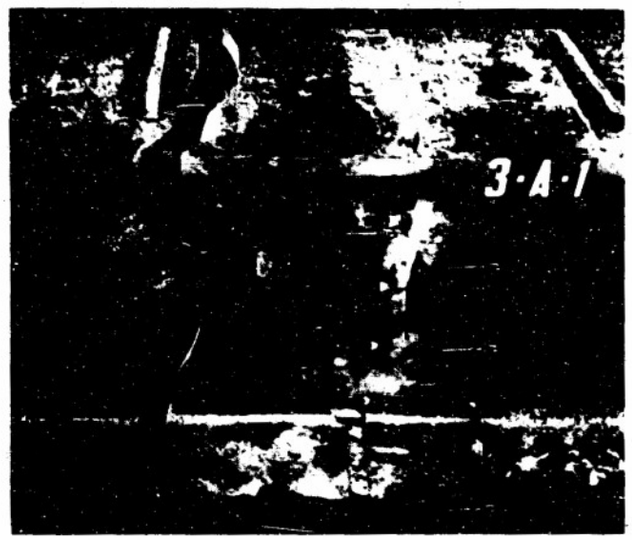

Plate 15 SK beam 3 A1 stress relieved, tested at −124° F. Crack started at angle fixture weld on top flange and extended through base metal. Test discarded

STRAIN RATES

Strain rates produced by impact are not easily evaluated, particularly when flexural strains are involved, both elastic and inelastic, and local discontinuities produce indeterminate local concentrations. Even in the case of simple tension impact, the strain rate at the instant of fracture cannot be determined from the striking velocity, except that a reasonable approximation can be made when the specimen breaks without appreciable plastic deformation with a small expenditure of energy and little change of velocity of the striking mass occurs during the essentially elastic fracturing operation. Under flexural impact loading, the inertia effects, subimpact phenomena and effects of discontinuities further complicate the problem.

In the loading operation, a force (stress) is applied at a particular rate. The deformations are at first essentially elastic. When the stress reaches the yield point, the stress remains constant until considerable plastic deformation has so altered the properties as to require an increase of stress to produce further deformation. Throughout the "yield" range, the elastic strain component remains constant and only the plastic component increases. The elastic strain rate is zero in the yield range. When strain hardening develops increasing the stress required to continue deformation, the rate of increase of the elastic component is low even though the rate of plastic deformation may be high. Since it is the limiting internal force (stress) which determines fracture, the amount of plastic strain preceding fracture is important only in so far as it has altered the resistance of the material at the particular temperature. It is the rate of application of the elastic strain component which is significant in the dynamic fracturing operation, rather than the total strain rate. The magnitude of the internal stress and its rate of application, both of which are proportional to the elastic strain component, together with the properties of the material existing at the test temperature, determine the character of fracture.

A typical strain and corresponding deflection transient taken from one of the film records is shown in Fig. 19. The upper transient represents the strain on the weld at midspan of the lower flange surface. The strains in the web at the curved surface of the hole follow an almost identical pattern, differing only in magnitude. Strains at other locations, recorded simultaneously, are not shown to avoid confusion. The lower transient represents the deflection at midspan. This record was for a 30-in. drop on an SK beam tested at 0° F. No permanent sets were produced at this blow.

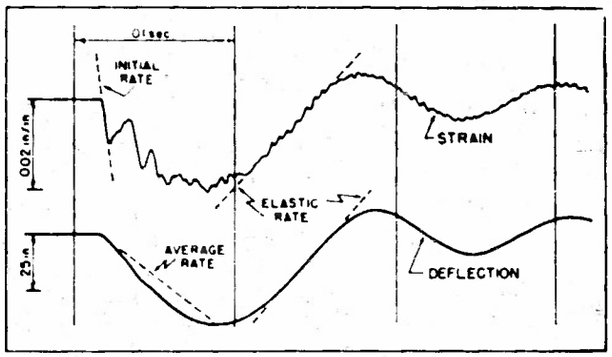

Fig. 19 Typical strain and deflection transients

The irregularities of the strain pattern reflect the superimposed effects of beam curvature, subimpact and stress waves. The deflection curve is the integrated effect of strains throughout the beam and is not sensitive to the local strain variations. The initial strain rate, immediately after contact of the tup, represented by the slope of the first serration in the strain pattern, is of the order of 4.5 in./in. sec and reaches higher values for greater heights of fall. The magnitude of the strain reached at this high rate is about 50% of the maximum strain produced by this blow. Obviously this strain is not related to the over-all beam curvature which is associated with a very small deflection in this period of time. At the instant of fracture, these vibrations would be damped by the plastic deformation accompanying the fracturing process and probably do not add appreciably to the elastic strain at fracture. Referring to the free vibration cycles after the first forced deflection of the beam, the localized strain variations indicated by the ripples superimposed on the mean curve diminish in intensity with the natural damping of the beam deflections. Similar patterns for the strains at the hole where plastic deformations are produced at an early stage are much smoother after the forced cycle.

The mean slope of the upward recovery portion of the first cycle represents the elastic strain rate due to beam action. Comparing this rate for the flange strains with that determined for the strains measured on the curved surface of the hole, it was found that the strain rate

at the hole was about two times the rate on the flange. Since the strain increments occur in the same time, this means that the magnitudes of the strains were in the same ratio. This agrees with the direct measurements made in the static tests.

Except for some of the fractures which occurred at the lowest temperatures, with relatively small heights of fall of the tup, the tension gages were broken by excessive strains before fracture and the strain rates had to be approximated from the available deflection record. The rate of the deflection recovery is consistent with the elastic lower flange strain rate record when converted by the elastic relation between deflection and strain. This is true also when the blow produced large permanent deflections indicating elastic action during recovery and justifying the approximation of elastic strain rates, with a concentration factor of 2 from the deflection records. In general, the fractures occurred after appreciable plastic deformation and the total measured deflections include both elastic and plastic components. However, due to the shape of the stress-strain curve for this material in which the stress remains essentially constant in the yield range, the elastic component of the deflections probably does not increase greatly beyond the value at the flexural proportional limit. Converting the elastic deflection rates to strain rates at the hole, the maximum strain rate produced in these tests is of the order of 0.90 to 1.0 in./in./sec for beams which developed structural yielding. For beams tested at −115° F which broke in the elastic range, the strain rate was about 0.80 to 0.90 in./in./sec. The time to maximum strain and deflection was 0.007 sec.

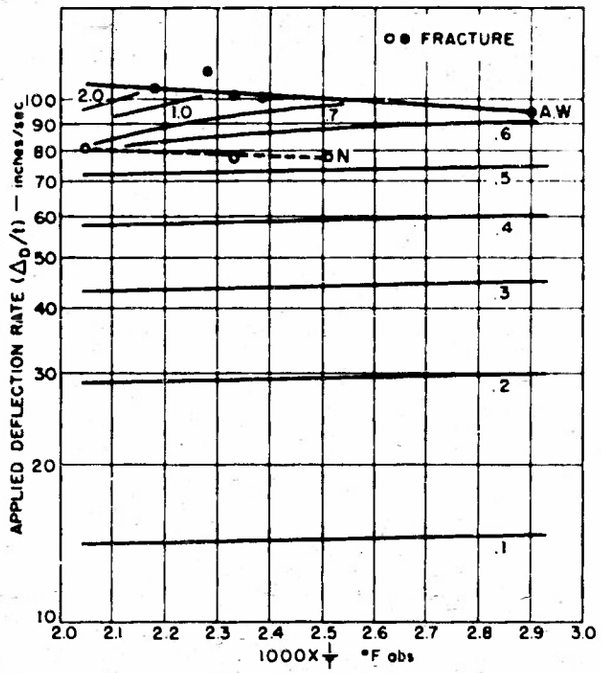

Fig. 20 Dynamic deflection rate at indicated total deflections and fracture, Semikilled steel

A. W.—Fracture curve for as-welded beams. N—Fracture curve for beams with Pressed Notches. Numerical designations—Total beam deflections including sets.

As a further study of the straining rates at various temperatures the data shown in Figs. 20 and 21 were derived from the dynamic deflection records. The average deflection rate $\Delta d/t$ is taken as the slope of the line drawn from the starting point of the forced deflection cycle to the point of maximum dynamic deflections. This average slope is probably a fair approximation of the rate of the elastic component, particularly when large sets are produced, and $\Delta d/t$ can be taken as a measure of the strain rate. The variation with temperature of the deflection rates to produce a given deflection are shown by the lines representing increments of deflection, Δ = 0.1, 0.2, etc. The deflection rate to produce a given deflection appears to increase slightly, about 5%, with decreasing temperature over the range of these tests (−115 to +30° F). Deflections lower than about 0.50 in. represent elastic action, without permanent set. This change in deflection rate suggests some effect of temperature on the properties of the material, possibly the damping capacity.

The deflection rates, i.e., strain rates at fracture, decrease with decrease of temperature (about 12%). These average deflection rates reached maximum values of 120 to 130 ips. The fracture points for beams with pressed notches, to be discussed later, are also shown. That the deflection rates to fracture are smaller than the welded beams with holes indicates a greater concentration factor and strain at the sharp notch as compared with the web hole. The data are limited for the purposes of these comparisons because the investigation was planned primarily to determine transition temperatures and most of the tests were concentrated within this critical range, which does not provide sufficient data for a more extensive analysis of strain rates.

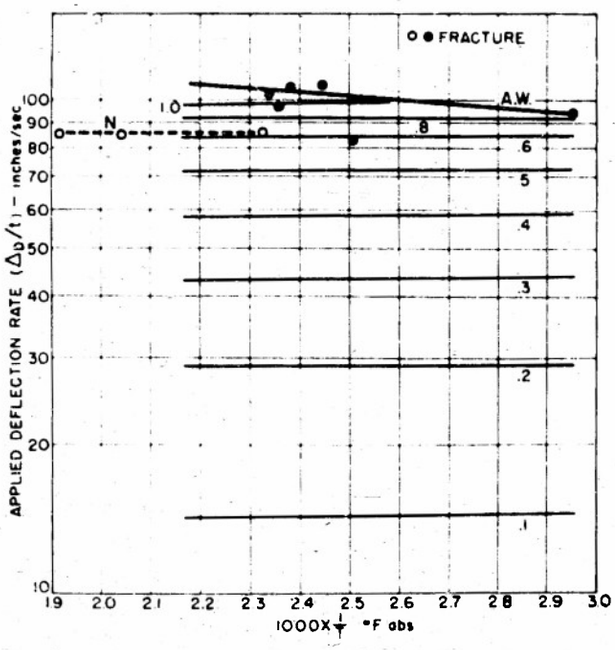

Fig. 21 Dynamic deflection rate at indicated total deflections and fracture, fully killed steel. See legend, Fig. 20

Deformations at Failure

The deflections of the beams at fracture or when the tests were discontinued due to buckling are shown in Table 5. These total deflections, including permanent sets, reflect the integrated deformation of the entire beam. Local strains were measured with electric strain gages on many of the beams, but these gages were broken in most cases long before ultimate failure of the beam. To obtain some measure of the maximum strains developed prior to failure, fine scratches were scribed on the tension flange surface and on the web directly over the hole. These scratches were made at $\frac{1}{10}$ in. intervals over a length of 3 in. On the flange, two longitudinal gage lines, $\frac{1}{4}$ and $2\frac{5}{8}$ in. from the edge were placed symmetrical with midspan, thus including the weld and extending beyond the boundaries of the web hole. The web gage line was about 0.04 in. above the edge of the hole at midlength. Distances were measured between scratches with an optical micrometer having a minimum reading of 0.0001 in.

These measurements give some indication of the amount of plastic strain developed prior to fracture. The strain associated with the fracturing process, being very local and included in a scratch interval lost by the fracture, could not be determined. Figure 22 shows typical plots of the measured strains, based on $\frac{1}{10}$-in. gage lengths for two beams which buckled without fracture. Beam 5E1 was FK unwelded with a drilled web hole, tested at $-112°$ F, developing a center deflection of 1.20 in. Beam 2E was SK, as-welded, tested at $+10°$ F and developed a center deflection of 2.53 in.

A summary of the data for all beams shows a marked decrease of plastic deformation preceding fracture with decrease of temperature, in both the flange and web at the hole. These variations in the flange are from about 0.2% at $-115°$ F to 8% at $+30°$ F, with a tendency for the edge strains to be smaller than those closer to the web line, particularly at the lower temperature. On the web over the hole the strains varied from 0.2% at $-115°$ F to 26% at $+30°$ F. The lower value is the limit of accuracy of the measurements. The strains on the curved edge of the hole were probably somewhat larger than those recorded above the hole.

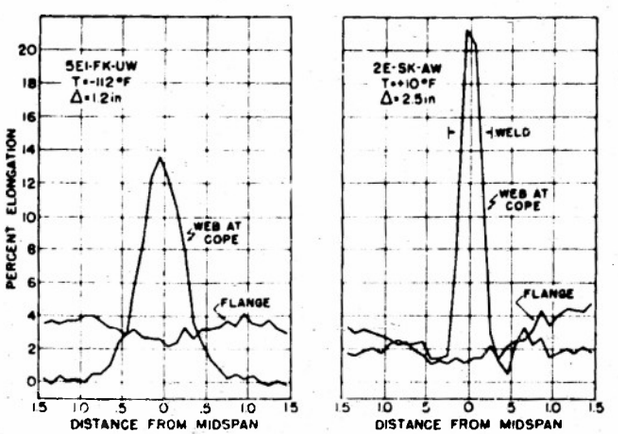

Fig. 22 Deformations in flange and web

PREPARATION OF WEB HOLES

During the progress of the impact tests, it was apparent that the presence of the web holes which, in effect, formed an internal notch, introduced a critical condition for the initiation of cracks. In addition to the geometry factor, the web weld terminated at the hole and the holes were finished to shape by flame cutting after welding, in order to remove imperfections at the "run-out." The strain concentration at the hole and the relative plastic behavior of the weld and base metals have been discussed. The possible effect of the flame-cut finishing operation on the initiation of cracks, was questioned and a few supplementary tests were made to provide some information.

Four unwelded beams, as-rolled, were provided with web holes, simulating those used in the welded beams, by piercing the web and shaping to size by oxy-acetylene flame. This piercing operation introduced more local heat than the finishing after welding with the likelihood of inducing greater residual stresses and the edges were somewhat more irregular due to the difficulty of using the torch so close to the flange surface. The residual stresses induced are not likely to have contributed to the failures since plastic deformation preceded the fractures. Four beams of each of the two materials were tested under impact at various temperatures. The results are recorded in Table 5. The FK beams fractured with cracks starting at the holes, at or below $-40°$ F and buckled at $-20°$ F, suggesting a transition temperature of about $-30°$ F which is the same as the as-welded beams. The SK beams fractured at $-115°$ F but buckled at $-60°$ F and higher. The temperature of transition from buckle to fracture is not closely defined because of the limited number of specimens but it is apparent that the preparation of the holes had an unfavorable effect since beams tested with drilled holes buckled without fracture at $-115°$ F. A comparison of the behavior of the two steels is not justified by these few tests. The effects of manual flame cutting are likely to be variable, particularly with respect to roughness of the finished edge and accidental gouging. Two of the FK beams cracked in the flange only, at the edge of the hole, which was unusual.

It was not the purpose of these tests to investigate the physical and metallurgical aspects of flame cutting, but in view of the above results, an examination was made of flame-cut edges at the hole. Samples were taken from four previously tested welded beams, which had cracked at the hole adjacent to the tension flange but finally buckled. The samples were taken at the upper hole where the material had been subjected to stress but was uncracked. Plate 16A shows micrographs, originally taken at 500 ×, of the edge of the base metal, outside the welding heat-affected zone, from a FK beam. Both steels showed similar conditions. Plate 16*B* is a micrograph, from the same specimen, originally taken at 1000 ×.

Plate 16A shows multiple surface cracks existing in a hard transformation layer (white) having an average

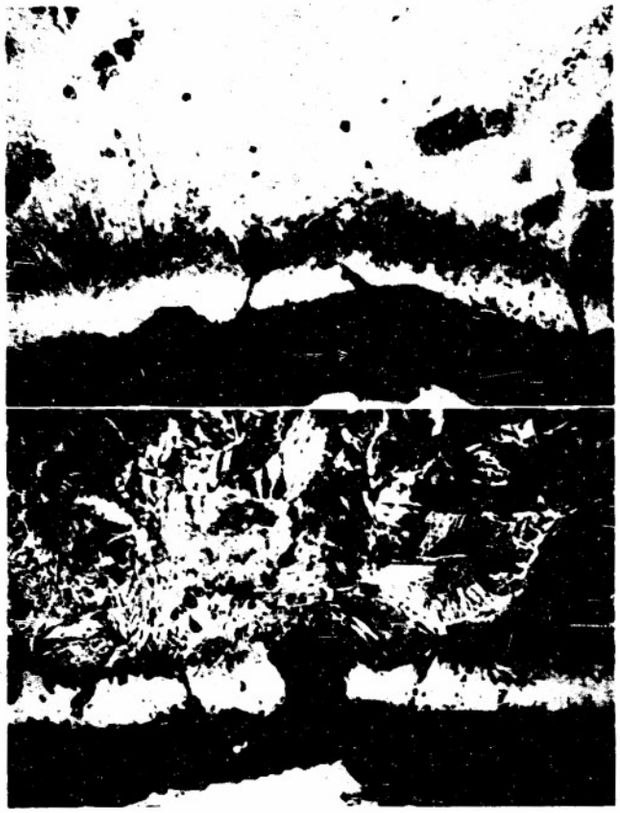

Plate 16A Micrographs of flame-cut edge of base metal at hole

depth of about 0.0015 in. and an average hardness of Converted Rockwell "C" 32. It will be noted that oxide has penetrated into the cracks. The structure back of the hard transformed layer consists of a typical overheated steel structure to a depth of perhaps $\frac{1}{16}$ in. Plate 16*B* is a further illustration of multiple cracks in a hard transformation layer at the flame-cut edge. The cracks are included in a hard and more brittle material tending to terminate upon entering into the relatively softer overheated zone having an average hardness of Converted Rockwell "B" 95. These hardness measurements were made on a Bergsman Micro Hardness Tester employing a 5-g load. The presence of oxide in these

Plate 16B Micrograph of flame-cut edge of base metal at hole

cracks indicate that the formation was associated with the heating cycle, not due to subsequent load stresses and represent thermal cracks probably developed during the rapid cooling.

The shallow cracks at the flame-cut edges are stress raisers, which should invite the initiation of major cracks whose propagation depends on the properties of the base metal at the test temperature. It should be noted that in preparing the beams for impact test, the upper edge of the lower hole, including the weld and adjacent base metal, was smoothed with a file for gage placement. This filing probably removed the shallow cracks present at the critical region but may not have removed the heat-affected zone. The corners of the hole adjacent to the flange surface were not filed. In some cases a shallow gonged groove was produced by the cutting at the corners, which together with the edge condition and the discontinuity produced by the hole produced a critical region in the flange, where some of the fractures did occur.

While the edge effects of flame cutting are unfavorable at a stressed edge subjected to high strain rate at low temperatures, the tendency to crack propagation is reduced at higher temperatures by the higher energy absorbing capacity of the base metal. Other reported tests indicate the visible start of cracks at flame-cut edges to be independent of the temperatures used or type of subsequent fracture, and higher fracture stress for smoothly ground surfaces[3] under static loads. Also the effects of flame cutting in preparing the edges for welding are unimportant because of the subsequent fusion by the welding operation.

In the type of splice tested, the web holes were considered necessary to facilitate the flange welding. What would have been the result if no holes were present, assuming that a sound weld could be made, or could the shape and formation of the hole be modified to improve the beam behavior at low temperature? To answer the first question, a few additional tests were made in which the splice was made by continuous welding of the web and flanges without web holes. A trial weldment indicated apparently satisfactory weld soundness and the practicality of the procedure.

Assuming that the holes are necessary for fabrication, why not fill the holes with weld metal after completion of the splice, thereby removing the stress concentration and edge effects of flame cutting? This procedure was considered but rejected because of the danger of imperfections which might be more unfavorable than a well-formed hole. The remaining alternative then concerns the best method of forming the hole. The suggestion has been made to elongate the hole in the direction of the flange, thus reducing the curvature of the edge facing the web and moving the flange strain concentration further from the weld zone. The hole might also be enlarged without seriously reducing the web strength.

Practical considerations require that web holes, whatever their shape and size, be formed by flame cutting. Although the presence of microcracks at the cut edges would not be eliminated by postheating, such

treatment would tend to improve the properties of the heat-affected edge zone with less likelihood of propagation of these shallow cracks at temperatures above the critical propagation temperature of the material. It will be noted that beams of both steels were tested after stress-relief treatment following fabrication. This postheating of the entire beam to 1150° F produced no change in the transition temperature of the SK welded beams as compared with the as-welded conditions. Some improvement was produced in the FK beams. It is not clear, however, that the relative behavior due to this post heat can be attributed to any influence of flame-cut edges of the welded beams.

The alternate fabrication procedures which have been discussed in view of the findings of these tests are of interest to the designer and warrant further trial and study. Some tests were made on beams spliced with a continuous weld without web holes for comparison with the beams of the original program. The results are recorded later in this report.

CRACK PROPAGATION

In the previous discussion of the fractures produced, it was indicated that the extent of the cracks varied with the test temperature. At temperatures well below the transition to buckling, shattering failures resulted with branching cracks extending laterally in the web and through the upper flange. At somewhat higher temperatures the cracks did not include the upper flange, diminishing until only part of the web cracked. At the threshold of transition, cracks at the web hole reduced to short tears which did not propagate even when impact loads were increased to ultimately produce buckling.

The extent of the cracked section, expressed as a percentage of the depth of the section and plotted as a function of the test temperature, is shown in Fig. 23. No attempt is made to include the exact length of branching cracks, which sometimes extend a considerable distance in the web, or to assign relative weights to web and flange cracks. The curves should terminate at temperatures producing no crack, corresponding to the transition temperature according to the crack-buckle criterion. Beam specimens are not suitable for a study of crack propagation. It will be noted that partial fractures tend to terminate at midheight or slightly above, where the flexural stresses are low or the crack enters a compression field. The results do, however, suggest a relation between the extent of crack propagation and temperature. The web cracks in the welded beams were usually in or adjacent to the weld metal. To further investigate the effect of temperature on the extent of free-running cracks without welding complications, a few unwelded beams were prepared with sharp pressed notches at the top of a drilled web hole. Retaining the geometry of the welded beams the notch served as a crack starter in the web. The tool used to form the notch was ground to a sharp edge which was slightly rounded on polishing paper. In order to minimize upsetting of the material by pressing the notch, a notch slightly undersize was first formed with a file. Pressure on the inserted tool then shaped the notch to its final contour. Plate 17 is a micrograph of a section taken through the notch at about mid-thickness of the ½-in. web material. Only a slight distortion of the structure is noticeable at the root of the notch. From measurements of this micrograph, the radius of the root was 0.00075 in. The notches were 0.1 in. deep (above hole edge) with 45-deg included angle.

Three unwelded beams of both as-rolled materials with pressed notches were tested under impact at different temperatures. Due to the limited number of tests with only the welded beam results to predict per-

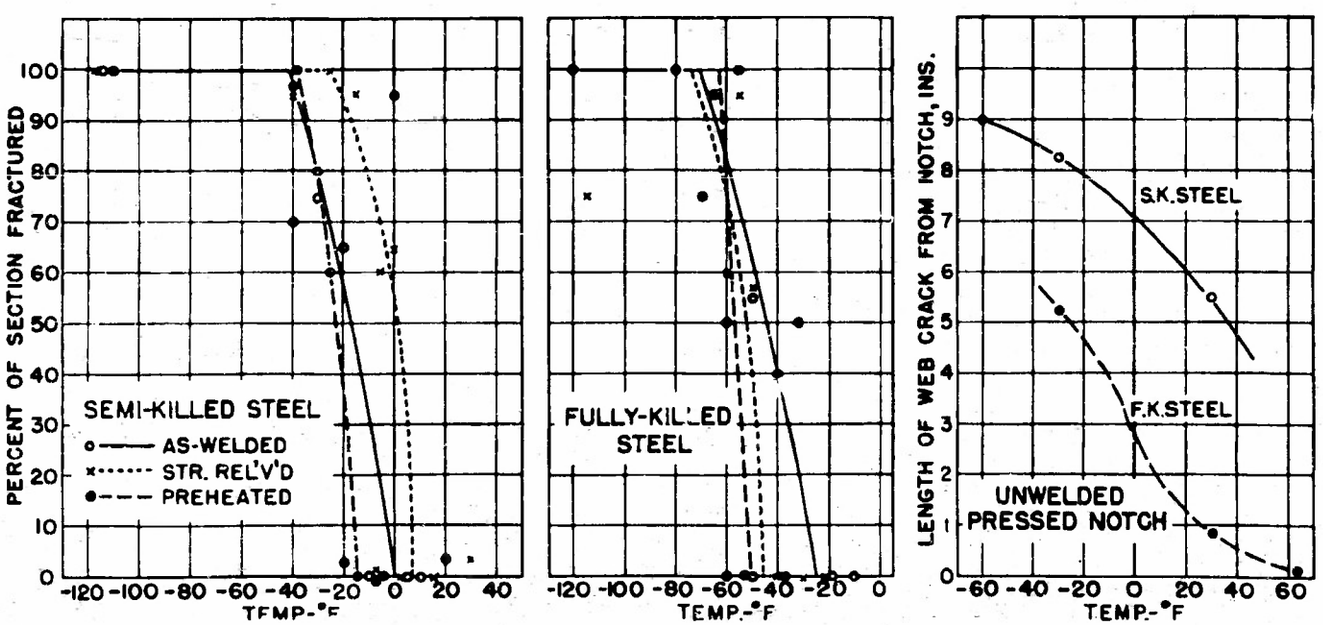

Fig. 23 Progress of cracks in beam section with temperature

Plate 17 Micrograph at root of pressed notch used as crack starter

formance, the temperature range of the tests is rather wide, but the results indicate a decided difference in the tendency to permit free-running cracks in the two materials. The test data are shown in Table 7. The lengths of the initial cracks originating at the notch

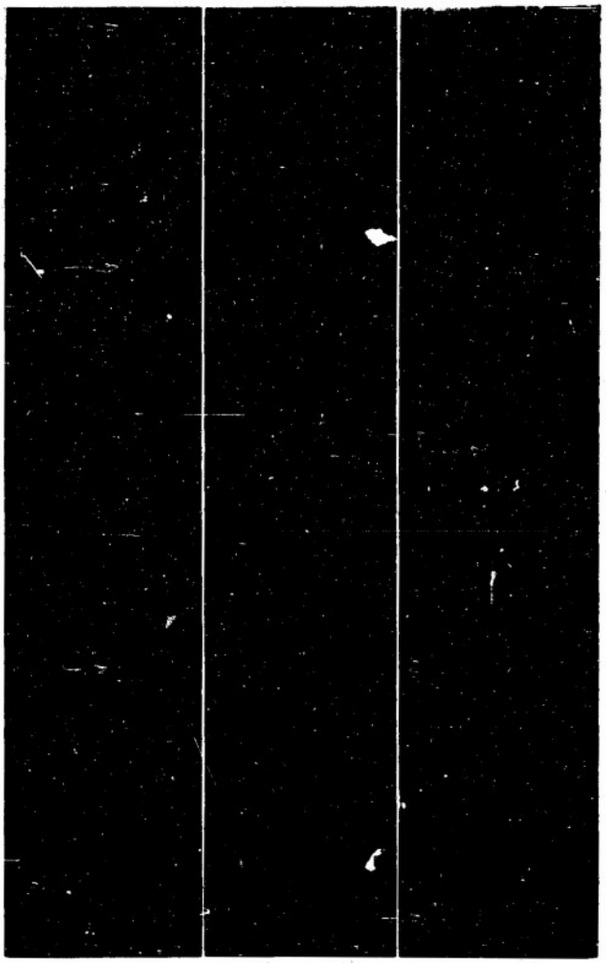

Plate 18 Fractures in unwelded and notched beams, SK series

Table 7—Propagation of Cracks Induced by a Pressed Notch

Mark	*Steel*	*Test temp., ° F*	*Drop at crack, in.*	*Beam deflection, in.*	*Strain energy to crack, ft-kips*	*Length of crack, in.*	*Fracture*
2C1	SK	−60	48	0.60	6.4	9	Granular
3B1	SK	−30	42	0.53	5.3	8 1/4	Granular
3B	SK	+30	42	0.60	6.2	5 1/2	Granular
2D1	FK	−30	54	0.69	7.5	5 1/4	Granular
3D	FK	+30	48	0.66	7.6	1/2–7/8	Granular (see note below)
2D	FK	+63	54	0.91	11.7	1/16	Fibrous

Specimen 2C1, SK at −60° F. The fracture is rough granular with chevron pattern pointing toward the notch over the lower 7 in. changing to fine granular near the end of the crack. No measurable change of thickness occurred over the entire length. Sectioning of web, at the end of the crack, showed that the crack advanced further in the center of the web thickness (0.485 in. thick) by 0.10 in. as compared with end of crack at the web surfaces.

Specimen 3B1, SK at −30° F. The entire fracture is fine granular with chevron pattern on the lower 5 in. Thin silky lips at the edges in the upper 2 in. extend about 0.02 in. deep. No lips were near the notch. No measurable change in thickness occurred near the notch but the thickness decreased by 0.003 to 0.010 in. adjacent to the crack over its upper length. The granular fracture was finer at the terminating end.

Specimen 3B, SK at +30° F. The web surfaces along the line of the entire crack were necked on both sides to reduce the thickness by 0.025 in. with a small dimple at the terminating end. Within this necked zone, the fracture extended to the surfaces as a fine crack for about 4 in. from the notch. This fracture was rough granular with a chevron pattern pointing to the notch, except for surface lips extending along the entire length (including part near notch) which were about 0.02 in. deep. These lips were smooth shear fractures. The fracture in the upper 1 1/2 in. of its length was *internal;* not extending through the neck at the surfaces. (See Plate 18) The section remaining intact was about 0.02 in. deep.

Specimen 2D1, FK at −30° F. The fracture was rough granular with chevron pattern. Edge lips are 0.01 deep near notch and 0.02 in. deep further away. No appreciable change of thickness occurred near the notch, but the thickness decreased 0.01–0.02 in. in a narrow necked zone. The crack terminated in a dimple.

Specimen 3D, FK at +30° F. The first crack was 1/2 in. long at the 48-in. blow. The crack extended to 7/8 in. long at the 84-in. blow when the beam ultimately buckled. The fracture is granular with smooth edge lips. The crack terminated in a dimple or depression where the thickness decreased 0.065 in. (original 0.485 in.).

Specimen 2D, FK at +63° F. A small tear, 1/32 in. long, formed at the notch at the 54-in. blow. This crack became 1/16 in. long at the 84-in. blow when the beam buckled. The crack formed at 45 deg to the vertical through the notch. The fracture appears rough fibrous. A dimpled zone at termination had a thickness reduction of 0.045 in.

and extending vertically into the web are shown graphically at the test temperatures in Fig. 23.

The cracks developed in the SK series are shown in Plate 18. In the view of Specimen 2-C-1 (−60° F), the surface adjacent to the crack is not visibly changed. (The scribe line, vertically from the notch, is not to be confused with the cracks in these views.) The surfaces adjacent to the fine crack in Specimen 3B1 (−30° F) is slightly depressed. Plastic deformation is suggested by the lighter zone along the crack. The view of Specimen 3B (+30° F) shows a pronounced local decrease in thickness along a vertical line starting at the notch. Close examination showed a very fine crack in the root of this necked-down zone over the lower 4 in. of its length. The internal condition is discussed more fully below.

Plate 19 shows the crack formations in the FK series. Specimen 2D1 (−30° F) showed a small and narrow localized necking at the crack. The short crack above the notch in Specimen 3D (+30° F) did not propagate beyond its initial formation with subsequent blows which produced considerable deformation of the web as evidenced by scaling and strain lines. The crack terminates in a pronounced depression or dimple. The smaller crack in Specimen 2D (+63° F) is more properly described as a tear which did not propagate with subsequent blows.

The fractures near the notch of Specimen 3B, SK tested at +30° F and specimen 2D1, FK at −30° F are shown in Plate 20. The smooth lips at the edges

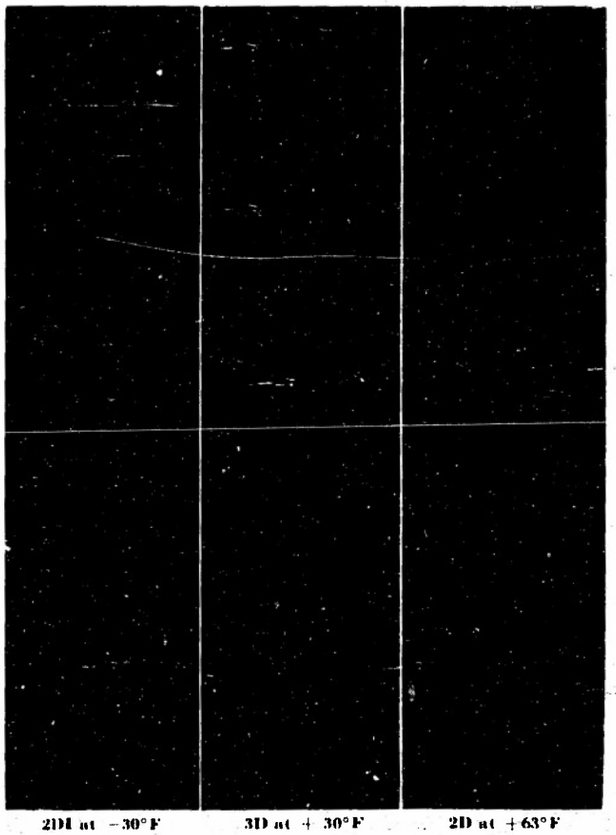

2D1 at −30° F 3D at +30° F 2D at +63° F

Plate 19 Fractures in unwelded and notched Beams, FK series

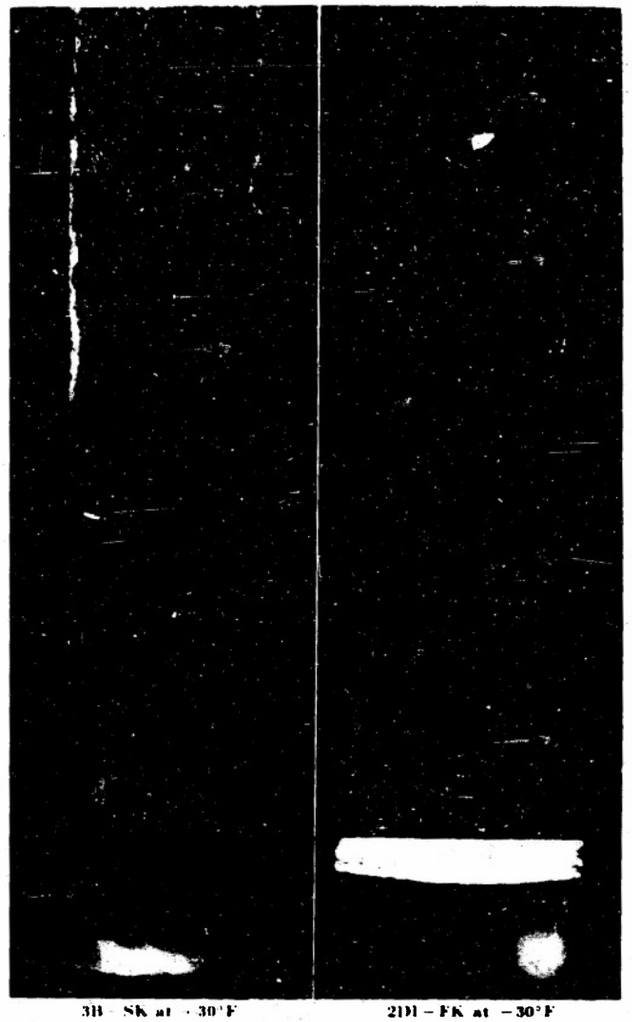

3B—SK at +30° F 2D1—FK at −30° F

Plate 20 Fractures near notch of specimen, edges show smooth lips

are visible as lighter zones. The fracture of Specimen 3B provided interesting information concerning the formation of these cracks. The web surfaces along the line of the entire crack were necked in on both sides. Only after close examination was a very fine crack found at the bottom of the narrow necked zone over the lower 4 in. of its length. The appearance of this fracture is shown in Plate 20. A section cut through the thickness of the web where the surface was necked without visible surface crack, showed that the crack was *internal* leaving the material intact near the original surfaces for a depth of about 0.02 in. This internal fracture is shown in Plate 21*A*. It is this thin surface zone which when ruptured shows a smooth shear fracture and forms, what has been called a "shear lip," at the edges. In Plate 21*A*, the view includes the full thickness of the web across which the crack extends. One edge clearly shows the necked-down surface. The opposite surface had been ground and polished for etching, which removed the depression similar to that on the other surface. This polished surface, after Fry etching, is shown in Plate 21*B*. The etching (dark zones) shows plastic deformation in a zone about $\frac{1}{8}$ in. wide along the entire crack starting at the notch. At

the termination of the crack the branching strain lines indicate dissipation of energy by shear deformation ahead of the crack.

Similar etching of Specimen 3B1, SK at −30° F showed no appreciable plastic zone adjacent to the crack but a few branching strain lines spread out beyond the end of the crack. The etching process was not effective on any of the FK specimens.

The condition near the terminating end of the crack formed on Specimen 2C1 SK at −60° F, was examined by sectioning the web. At the center of the web thickness (0.485 in.), the end of the crack had advanced 0.10 in. ahead of the end of the crack at the surfaces. This suggests faster-propagation at the center, with a lag and modified fracturing force on the section nearer the edges which may be associated with the irregularities of the fracture surface referred to as chevron or herringbone. The presence of a lip at the edges of a fracture can also be interpreted to indicate prior internal fracture. Whether this condition is due to the propagation phenomena or different properties of the material, such as a skin effect, at the surfaces of the rolled plate is not indicated by these data.

Referring to the data in Table 7 and Fig. 23, both series of tests indicate that the tendency for crack propagation decreases as the temperature is raised. In each series composed of three tests, the striking velocity, beam deflection and hence the strain rate at the root of the notch, when fracture occurred, was nearly the same. The initiation of cracks at the notch appears therefore to be independent of temperature over the range of 90° F in these tests. The length of crack, however, is primarily related to the temperature. Comparing the two series, the cracks were initiated at lower strain rates on the SK steel. The tendency to propagate the crack, as measured by its length, at the same temperature is also more pronounced in the SK steel. The crack length in the SK steel at +30° F (with lower initial strain rate) was about the same as that in the FK steel at −30° F, a difference of 60° F. In the FK series, the cracks initiated at the higher temperatures did not propagate with subsequently increased impact loads and the ability of the beams to resist loads up to normal buckling refusal was not impaired.

It appears that above some critical temperature, cracks do not propagate. The lowest temperature inhibiting free running cracks is a more rational and useful definition of transition temperature than one based on factors related to the initiation of a crack or physical characteristics of the fracture itself, which.

Plate 21A Internal fracture of web of Specimen 3B, SK +30° F. Note necked-down and intact surface

Plate 21B Surface of web at termination of crack which does not extend through necked surface. Dark zones produced by Fry etch indicate plastic deformation

however, may reflect the propagation phenomena. From a practical viewpoint, the presence of small cracks, produced by fabrication or erection processes, which are known to exist, do not in themselves impair the serviceability of the structure. They do, however, serve as a starting point for extension when the stress intensity and the properties of the material at the operating temperature are critical. It may be argued that without crack initiation, the question of crack propagation is irrelevant and suitability for service is thus determined by the temperature at which cracks start thereby introducing a propagation potential. However, it affords little assurance to delay cracking by a few degrees if the crack, once started, leads to complete destruction of the member, as would be the case in a material lacking propagation toughness.

While the data are too limited to warrant quantitative comparisons, the curves in Fig. 23 are displaced by about 60° F. Assuming that the curves are nearly parallel when the SK curve is continued to a nonpropagating temperature, it could be concluded that the SK steel reached a critical temperature favorable to propagation about 60° F higher than the FK steel and that these temperatures are of the order of +25° F and +85° F, respectively. Recognizing that liberties are being taken with limited data, these temperatures and their difference are in fair agreement with the transition temperatures derived from the V-notch Charpy tests at the 50 ft-lb level, for the specimens taken near the fillet and adjacent web (see Table 3, locations 3 and 5) but bear no relation with the results of the keyhole-notch Charpy tests.

LOW-HYDROGEN ELECTRODES

The beams for the major series of tests in which as-welded, stress-relieving and preheat treatments were investigated were butt welded with E6011 and E6020 electrodes. The results showed lower transition temperatures for the FK steel. It was of interest to determine whether the use of low-hydrogen electrodes would improve the performance of both steels, whether these electrodes with SK steel would accomplish the same result as using FK steel as originally welded and whether the advantages of preheat might be duplicated.

One series of tests was made on beam specimens butt welded with E6016 electrodes (without moisture control) including both steels, as-welded and with preheat. No change of welding procedure was made other than to use d-c reverse polarity current instead of the 25-cycle a-c current used in the original series. The electrodes were used out of fresh boxes as received from the storage room. It is important to note that no attempt was made to control the moisture content of these electrodes.

To determine the influence of moisture control a second series of tests was made on specimens welded with E6016 electrodes conforming to Grade MIL-E-180-16, Federal Specification MIL-E-986A. These electrodes were packaged in 40-lb hermetically sealed containers, which were opened as required and the electrodes were placed in an electric oven at a temperature of 250° F. Electrodes remained in the oven overnight before being used the following day. All welding was done on the day shift. The welder took only enough electrodes out of the oven to last him 4 hr or less. At the end of the shift all unused electrodes were put back into the oven. This series included only FK steel beams (SK beams unavailable). Four specimens were provided for test as-welded and also when welded with preheat.

The results of tests on specimens fabricated with both types of low-hydrogen electrodes are recorded in Table 8 giving derived data similar to that shown in Table 5 for the original test series. The results are also shown graphically in Fig. 24.

The transition temperatures derived from these tests,

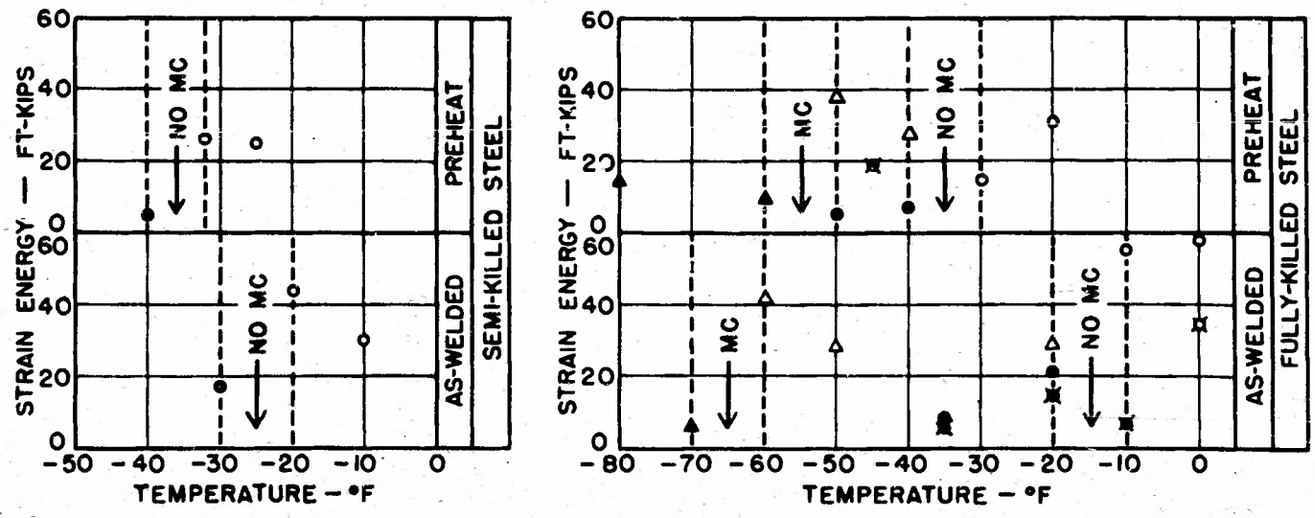

Fig. 24 Fracture-buckle transition temperatures, low-hydrogen electrodes, E6016

Table 8—Results of Impact Tests on Butt-Welded Beams, Low-Hydrogen Electrodes

Mark	Temperature, °F	Height of fall, in.*	Energy, ft-kips,†	Deflection, in.††	Equivalent loads, kips PL	Equivalent loads, kips YP§	Ratio, YP/PL	Stresses, ksi PL	Stresses, ksi YP	Failure
Semikilled steel, as-welded, E6016 electrodes (no moisture control)										
5C1	−30	78–108	17.0–51.2	1.10–2.75	210	260.5	1.24	65.2	80.9	Web fracture to complete
1B1	−20	108	44.3	2.43	190	250	1.315	59.0	77.6	Buckled
1B	−10	96	29.8	1.55	190	241	1.27	59.0	74.8	Buckled
						Avg	1.275			
Semikilled steel, preheat and welded, E6016 electrodes (no moisture control)										
3C	−40	42	4.7	0.50						Web and lower flange fracture
1E1	−32	96	26.5	1.59	218	255	1.17	67.8	79.2	Buckled
5B	−25	90	25.2	1.58	199	243	1.22	61.8	75.5	Buckled
						Avg	1.20			
Fully killed steel, as-welded, E6016 electrodes (no moisture control)										
5C	−35	42–72	5.6–16.7	0.55–1.10	202	244	1.21	62.7	75.8	Web and lower flange fracture**
7C	−20	66–96	15.2–36.1	1.05–2.22	185	238	1.29	57.5	73.9	Web fracture to buckle**
5C1	−10	48–70	7.2–25.3	0.64–1.61	182	230	1.26	56.5	71.5	Web and lower flange fracture**
4C1	0	96	33.8	2.12	167	228.5	1.37	51.9	71.0	Buckle**
2A	−35	48–60	6.8–11.6	0.61–0.72	232.5			72.3		Web to lower flange fracture
1A	−20	78	20.8	1.12	205.5	245	1.19	63.8	76.1	Web and lower flange fracture
4A	−10	110	54.6	2.98	178	234	1.32	55.3	72.6	Buckled
3A	0	110	57.9	3.49	167.8	224	1.33	52.1	69.5	Buckled
						Avg	1.28			
Fully killed steel, preheat and welded, E6016 electrodes (no moisture control)										
3A1	−15	78	18.8	1.10	200	258	1.29	62.1	80.1	Web and lower flange fracture**
2E	50	42	5.4	0.50	195			60.5		Bottom flange only (hole edge)
2A1	−40	48	6.8	0.61	217			67.4		Bottom flange only (hole edge)
4A1	−30	78	14.4	0.98	187	238	1.27	58.0	74.0	Buckled
1A1	−20	96	30.9	1.87	185	236.5	1.28	57.5	73.5	Buckled
						Avg	1.28			
Fully killed steel, as-welded, E6016 electrodes (with moisture control)										
2E1	−70	54	6.0	0.57	230			71.5		Complete fracture (small defect)
10B	−60	108	41.9	2.23	217	265.5	1.22	67.4	82.5	Buckled
10D	−50	96	28.6	1.66	210	253.0	1.21	65.2	78.6	Buckled
6E	−20	96	29.0	1.80	180	228.5	1.27	55.9	71.0	Buckled
						Avg	1.23			
Fully killed steel, preheat and welded, E6016 electrodes (with moisture control)										
10B1	−80	78	14.4	0.94	220	284	1.29	68.3	88.2	Complete fracture 6 in. from splice
6E1	−60	60	9.2	0.73	211			65.5		Web and lower flange
3D1	−50	102	38.0	2.15	208	256	1.23	64.6	79.5	Buckled
10D1	−40	96	28.3	1.72	190	250	1.32	59.0	77.6	Buckled
						Avg	1.28			

NOTE: See Table 5 for footnotes* to .
** Defective welds and gouged copes.

based on the fracture vs. buckle criterion, for the three types of electrodes used, are summarized in Table 9.

Referring to the series using E6016 electrodes without moisture control, the transition temperature was lowered for the semikilled steel by 20° F in both the as-welded and preheat conditions. Also the use of these 6016 electrodes on the SK steel in the as-welded condition produced about the same favorable effect as welding with preheat when using E6020 electrodes.

However, the use of these E6016 electrodes was unfavorable when applied to the FK steel in both the as-welded and preheat conditions. The critical temperature was raised by 15 and 20° F. When this unexpected reversal of effects on the FK steel beams was becoming evident during the progress of the tests, it was suspected that weld imperfections were responsible. Inspection of fractures disclosed some lack of fusion in the roots of the web welds. So as not to invalidate the conclusions concerning the electrode variable, additional beam specimens were fabricated and untested beams from the same lot were cut and rewelded with the two

Table 9—Effect of Type of Electrode on Transition Temperatures, ° F, of Butt-Welded Structural Beams

Type of steel, weld treatment	Type of electrodes: E6011, E6020	E6016, No moisture control	E6016, Moisture controlled
Semikilled			
As-welded	−5	−25	..
Preheat	−17	−36	..
Fully killed			
As-welded	−29	−15	−65
Preheat	−57	−35	−55

halves reversed so as not to introduce possible effects of previous welding. The results of tests on these replacements confirmed the previous tests, thus strengthening the conclusion that the transition temperature was raised and eliminating the suspected influence of weld imperfections. The lack of complete fusion, not found in previous weldments indicates that attention must be given to proper welding manipulation when using this type of electrode.

It has been recorded that the E6016 electrodes used for these weldments were taken from normal shop storage without special moisture control. An assumed unfavorable influence of moisture does not explain the inconsistency in behavior of the two grades of steel except that the electrodes may have contained different amounts of moisture, and the electrodes used for the SK series may have been more recently processed. The exactly opposite effect on the two steels might indicate that the combined properties of the steel and electrodes enter into the over-all behavior of the weldment in some indeterminate manner and a generalization as to the effectiveness of low-hydrogen electrodes, without moisture control, is not warranted.

A comparison of weldments with E6016 electrodes with moisture control is limited to FK steel since the supply of SK steel at this stage of the investigation was exhausted. These electrodes reduced the transition temperature in the as-welded condition by 35° F as compared with the same condition using E6020 electrodes. These electrodes apparently corrected the unfavorable influences of the E6016 electrodes originally used, presumably due to moisture control. However, when welded with preheat, the moisture controlled electrodes gave no improvement over the E6020 electrodes although they did avoid an increase of the critical temperature shown by the electrodes without moisture control. The results indicate that weldments with the moisture controlled electrodes as-welded are comparable to those fabricated with E6020 electrodes with preheat for the fully killed steel. In fact, these electrodes gave the most favorable results of any of the electrodes used.

These comparisons, based on the test results, give some information on the relative effects of the use of low-hydrogen electrodes with and without preheat. It is contended that hydrogen in combination with straining produces microcracks, which form during the rapid cooling after welding. Investigations with small specimens have shown that either preheat or the use of low-hydrogen electrodes will avoid microcracks, presumably because they both reduce the hydrogen content. Confirming this conclusion, these tests show that the critical temperature for beams welded with E6020 electrodes and preheat was about the same as for those welded with moisture-controlled E6016 electrodes as-welded, on the same steel (FK). If reduction of hydrogen content is the desired objective and both preheat and low-hydrogen electrodes are equally effective, then it would appear that, in welding the steel used in this investigation, no appreciable additive advantage would be obtained by preheating when using low-hydrogen electrodes. The limited number of tests on FK beams welded with moisture-controlled E6016 electrodes shows no improvement by using preheat over the as-welded condition.

The results of tests with electrodes having no moisture control (Fig. 24) appear contradictory to the above interpretation. However, these electrodes were not actually "low hydrogen" and the improvement shown by preheat treatment is consistent with the above reasoning. The effect on the critical temperature in either case, compared with the E6020 electrodes was not the same in the two steels. It should be noted that beam specimens were fabricated in lots at different times with the liklihood of different moisture contents in these uncontrolled electrodes. The moisture content was not determined because the effects were not suspected at the time of fabrication. While the preheat temperature was reasonably controlled for all specimens, the possible effect of varying this temperature under these conditions is not known. The interrelated variables of steel properties, electrodes, moisture control and preheat temperatures require further study.

WEB SPLICES WITH CONTINUOUS WELDS

A series of impact tests were made on six FK steel beams, butt welded without web holes. The electrodes used in these weldments were E6011 and E6020 to afford comparison with the extensive tests made on beams with web holes, in the as-welded condition.

The shop welding procedure for these splices is indicated in Fig. 25 and is briefly described as follows:

Preparation. The ends of the flanges and web of each beam were beveled by machine flame cutting to form a 60-deg, single-V welding joint with $^1/_{16}$-in. land and $^1/_4$-in. root opening. The flanges were beveled from the inside. At the corners where the web intersects the flanges, hand cutting was employed to insure a minimum opening of $^1/_4$ in. (see Fig. 25). Beams were assembled and tack welded on the outside of the flanges. The beam was positioned for each weld to permit welding in the flat position, except for short end returns as noted.

Web and Flange Welding. The sequence of the welding operation was as follows:

1. The web weld was completed first—refer to Fig. 25. The web root weld, W1 was made with $^5/_{32}$-in. E6011 electrodes. Subsequent web weld passes, W2, W3, etc., were deposited using $^3/_{16}$ in. E6020 electrodes to fill the groove. Each pass was started in the corner at the fillet and then run across the length of the web, ending in the opposite corner slightly above the fillet. The direction of welding was alternated first from left to right, then from right to left. The short end returns into the flange groove were made with the web passes while the web was in the horizontal position.

2. After the web bevel was completely welded, the

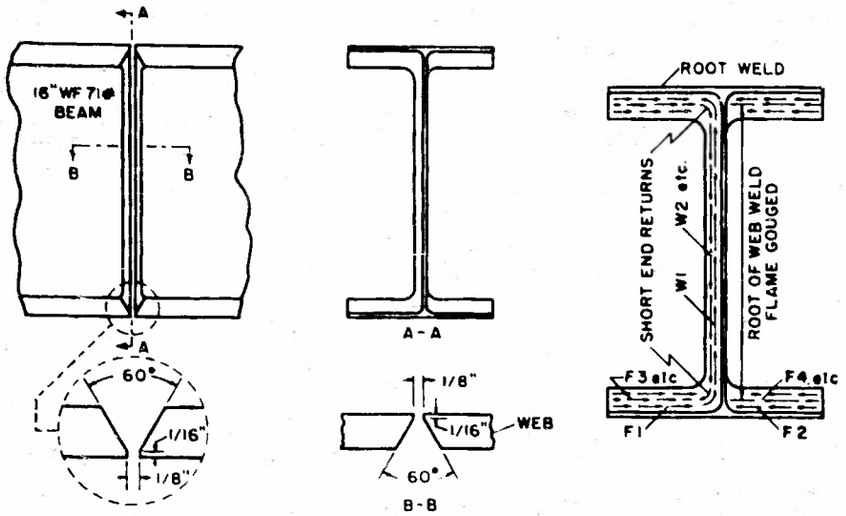

Fig. 25 Edge preparation and sequence of welding for butt welds without web holes

beam was turned over and the root was flame gouged to sound metal.

3. Two passes were deposited on the root side of the web weld using $^{3}/_{16}$-in. E6020 electrodes to complete the web weld.

4. Root passes, F1 and F2, on opposite sides of the web, in the first flange welded were made with $^{5}/_{32}$-in. E6011 electrodes. Subsequent passes on this beveled side were made with $^{3}/_{16}$-in. E6020 electrodes to fill the groove. All weld beads on the bevel side were deposited starting at the outer edge and progressing inward to the web.

5. After the bevel on this flange was completely welded, the beam was turned over and the root of this weld was flame gouged to sound metal. It was necessary to gouge deeply in the vicinity of the web-flange intersection.

6. Two passes were deposited on the root side of the flange using $^{3}/_{16}$-in. E6020 electrodes to complete this flange weld. These welds on the root side were run from edge to edge.

7. One flange was completed before starting on the other flange, which was welded in the same manner.

8. Outer ends of both flange welds were flame gouged to sound metal, rewelded and ground to the original beam contour.

The results of impact tests on these beams are summarized in Table 10.

The fractures developed in these welded beams without web holes are briefly described as follows:

Beam 9A (Tested at −60° F). The fracture was completely outside the weld zone. Starting in the lower flange, $2^{1}/_{2}$ in. from the centerline of the splice, the crack extended vertically in the web for about 9 in. and then branched toward the upper flange, which remained intact. The crack configuration was similar to that shown on Plate 14, with an additional crack branching to the right at the top. The texture was ragged to granular. As a possible explanation of the location of the fracture in the base metal remote from the welded splice, it should be noted that a rod for deflection measurement, previously described, was welded to the bottom surface of the flange. The flange fracture occurred through the outer edge of this localized weld zone. Although a deflection rod was similarly welded on the previously tested beams without apparent influence, it is possible that a detrimental condition existed which was made effective by the greater resistance of the continuous splice. However, Beam 9A1, also had a welded rod attached in the same manner and buckled without fracture at −40° F. Because of the possible influence of the welding of the deflection rod, all of the remaining beams were tested without deflection measurements. If the fracture was induced by the localized weld on the centerline of the flange without affecting the geometry, the cause was probably due to a metallurgical discontinuity producing a stress concentration.

Table 10—Impact Tests on Beams with Continuous Weld Splices

Beam No.	*Steel treatment*	*Test temp., ° F*	*Height of fall, in.*	*Permanent deflection set*	*Failure*
9A1		−40	90	1.15	Buckled
9E		−50	90	0.99	Buckled
9A		−60	84	0.54	Fracture, bottom flange and web
9B1	FK,	−65	96	0.91	Buckled
9B	as-welded	−80	33	0	Fracture, bottom flange and web
9E1		−90	21	0	Fracture, complete

Beam 9B (Tested at −80 °F). The fracture occurred in the weld metal of the flange weld and in the web weld to a height of about 3 in. The cracks then branched symmetrically in the web base metal, terminating at the upper flange fillets, leaving the upper flange intact. The crack pattern was similar to that shown on Plate 6, with the branch occurring nearer the lower flange. The fracture was fine grain around the beam fillet with the remainder ragged granular. The fracture apparently started at a V-shaped void $^{5}/_{8}$ in. long tapering from $^{3}/_{4}$ to $^{1}/_{4}$ in. wide located in the fillet zone. The surface of this void was oxidized by the flame gouging and indicates lack of penetration at the junction of the web and flange welds.

Beam 9E1 (Tested at −90° F). The complete fracture included both flanges and the web. The lower flange and lower 1 in. of the web fractured in the weld metal. The remainder of the web fracture and the upper flange fracture was about 2 in. from the splice.

The crack pattern was somewhat like Plate 9, except that the lower flange fractured through the weld and the web crack left the weld near the lower fillet. The lower flange fracture showed a small pinhole within an irregular texture indicating lack of complete fusion at the web-flange weld junctions.

In making this type of continuous web-flange welded splice, it was expected that some difficulty would be encountered in getting complete fusion in the fillet region. In order to determine the soundness of these welds, the welds were cut in a series of sections at both flange-web junctions of each of the six beams, after test. The findings of these examinations are:

Beam 9A1 (−40° F buckled). Bottom flange: No visible imperfections. Top flange: Single void $\frac{3}{16} \times \frac{1}{16} \times \frac{1}{16}$ in. deep.

Beam 9E (−50° F Buckled). No flaws in either flange weld.

Beam 9A (−60° F fractured). Bottom flange: Small pinhole. Top flange: Single void $\frac{1}{4} \times \frac{1}{16} \times \frac{1}{16}$ in. deep, located $\frac{3}{4}$ in. from centerline of web and $\frac{3}{4}$ in. from outside surface of flange.

Beam 9B1 (−65° F fractured). Bottom flange: Single void $\frac{1}{4} \times \frac{1}{16} \times \frac{1}{4}$ in. deep at mid-thickness of flange, $\frac{3}{4}$ in. from web centerline. Top flange: No visible flaws.

Beam 9B (−80° F fractured). Bottom flange: Flame gouged surface exposed in V-shaped void $\frac{3}{4}$ in. long tapering from $\frac{1}{8}$ to $\frac{1}{4}$ in. wide. Top flange: small pinholes in weld junction

Beam 9E1 (−90° F fractured). Bottom flange: $\frac{3}{16}$-in. diam hole in weld. Top flange: Single void $\frac{1}{8}$ in. diam $\times \frac{1}{16}$ in. deep in weld.

No defects were found in the fillet zone of the web weld.

Transition Temperature

Based on the fracture-buckle criterion, the data indicate a probability of failure by brittle fracture below about −70° F. This value neglects the fracture produced at −60° F because of the uncertainty of the effect of the subsequent localized weld in attaching the deflection rod and also neglects the effect of a sizable flaw in the weld of the beam tested at −80° F.

In any event, a comparison with the results obtained from the FK steel beams with web holes shows a decided improvement of performance. The continuous weld splice appears to have lowered the critical temperature by approximately 40° F.

The imperfections found in these welds are perhaps no greater than those frequently found in welds made under similar conditions, except for the sizable void found in one beam (9B). This unfused void does emphasize the need for special precautions in back gouging and back welding of the flange in making this type of splice which, however, should not introduce unreasonable limitations on the shop procedure.

The improved performance at low temperature of these continuous weld splices notwithstanding imperfections in the welds at the flange-web weld junction confirms the conclusion that the presence of web holes invited the start of cracks and thereby decreased the low-temperature resistance of the splice. The shop report and these test data justify the conclusion that the continuous weld splice is practical and preferred for low-temperature service.

SUMMARY AND CONCLUSION

The original objective of this project was the determination of the relative resistance and transition temperatures of structural steel beams, composed of SK and FK steels, fabricated with butt-welded splices and tested as-welded, after stress-relieving treatment and when welded with preheat. The results of this program of tests, the major part of which involved impact loading, suggested further investigation of welding and fabrication variables and these by-products furnish additional information on associated controversial questions. The analysis and interpretation of accumulated supplementary data contribute observations which are of interest in the design of welded splices and further study of the brittle fracture phenomena.

The findings are briefly summarized as follows:

1. Charpy tests on material taken from the rolled sections show a decrease of "notch sensitivity" by silicon-aluminum deoxidation. The Charpy values show a variation of about 20° F and 40° F for the SK and FK steels, respectively, depending on location in the rolled section. In the case of the FK steel, part of this variation was due to fissures developed transverse to the fracture. The material adjacent to the beam fillets in both the flange and web had the highest transition temperature. Comparisons at similar locations indicate lower transition temperatures for the FK steel by 50 to 75° F.

2. Impact tests on FK steel beams butt welded with E6020 electrodes show lower transition temperatures than the SK steel beams by 24° F in the as-welded condition and by 40° F after "stress relief" and when welded with preheat based on a fracture vs. buckle criterion. Welding with preheat was beneficial in both steels with E6020 electrodes, although to a greater extent in the case of beams made of FK steel. The results suggest the use of preheat on SK steel as an alternate to FK steel in the as-welded condition.

3. Strain measurements during both static and dynamic tests showed large strain concentrations in the vicinity of the open web holes introduced to facilitate the welding of the flanges. In most cases, fractures started at the web hole which acted as an internal notch, although at very low temperatures, fractures occurred in the base metal without regard to the splice.

4. Comparisons of the relative behavior of the welded beams was based on a fracture vs. buckle criterion. The extent of fracture varied with decreasing temperature from a small crack or tear at the web hole to complete shattering fracture of the entire section. At temperatures above those producing cracks, the beams failed by normal flange buckling. Test temperatures ranged from −120 to +60° F. The extent of the cracks produced showed a definite relation to the test temperature. A "shear lip" found at the edges of free-running cracks is associated with prior internal fracture.

5. The proportional limit and structural yield point of the beams under impact loading was determined

from derived equivalent static load-deflection curves. The proportional limit was reduced in these as-welded beams by residual stresses which were effectively minimized by stress-relieving treatment. The combined effect of decreased temperature and increased strain rate raised the elastic range of flange stresses to approximately double the static values at room temperature.

6. A limited number of tests on unwelded beams with drilled web holes in which a pressed notch served as a crack starter, showed a decided difference in the ability of the two materials to resist free-running cracks. The tendency to propagate a crack is more pronounced in the SK steel. To produce the same length of initial crack requires about 60° F lower temperature in the case of the FK steel. It appears that for the specimen and test procedure used in this investigation, cracks do not propagate above some critical temperature. The lowest temperature inhibiting free-running cracks is a more rational and useful definition of transition temperature than one based on factors related to crack initiation.

7. Static tests were inconclusive in determining resistance to brittle fracture at temperatures as low as −120° F. Under impact tests, brittle fractures were produced at temperatures up to 0° F. The strain rates produced in these impact tests were of the order of 0.8 to 1.0 in. in. sec. The time to maximum strain and deflection was about 0.007 sec, varying slightly with temperature.

8. Scratch measurements of deformation made after failure showed a marked decrease of plastic deformation preceding fracture or buckle with decrease of temperature, from 0.02% (limit of measurement) at −115° F to 8% in the flange and 26% in the web at the hole, at +30° F.

9. The presence of web holes introduced a critical condition for the initiation of cracks primarily because of the notch geometry involved. The finishing of these holes by flame cutting may have had some influence on the fractures particularly at the corners adjacent to the flange. Tests on unwelded beams with flame-pierced and finished holes showed transition temperatures approaching those of the welded beams. Beams with drilled and filed holes did not fracture at −115° F, the lowest test temperature. Examination of flame cut edges of the hole showed thermal cracks extending into the fusion zone about 0.002 in.

10. Tests of beams welded with low-hydrogen electrodes for comparison with similar beams welded with E6020 electrodes used in the major program, show:

(*a*) The use of low-hydrogen electrodes necessitates adequate moisture control and correct manipulation, if the best results are to be obtained.

(*b*) The E6016 electrodes used without moisture control were taken from normal storage. These electrodes, as used, on SK steel lowered the transition temperature by 20° F in both the as-welded and preheat conditions. The uncontrolled E6016 electrodes as here used on SK steel in the as-welded condition produced about the same favorable effect as welding with preheat and E6020 electrodes. Preheat was beneficial. It cannot, however, be concluded that the effect of preheat is superimposed on that normally expected with low-hydrogen electrodes because of the uncontrolled moisture content.

(*c*) The use of E6016 electrodes without moisture control was unfavorable when applied to the FK steel in both the as-welded and preheat conditions. The transition temperatures were raised by 15 and 20° F, respectively. The exactly opposite effect on the two grades of steel indicate that a generalization as to the effectiveness of E6016 electrodes as used in these tests is not warranted. It should be noted that the E6016 electrodes used in these weldments were taken from normal storage without moisture control and the moisture content may have been variable. The assumed unfavorable influence of moisture does not explain the inconsistency in behavior of the two steels, unless the absorbed moisture was unusually high in the case of the electrodes used for the FK steel beams first welded.

(*d*) A comparison of weldments made with E6016 electrodes with moisture control is limited to beams composed of FK steel. These moisture-controlled low-hydrogen electrodes lowered the transition temperature by 35° F as compared with the E6020 electrodes in the as-welded condition and apparently overcame the unfavorable effects of E6016 electrodes without moisture control. When welded with preheat the moisture controlled electrodes gave no improvement over the E6020 electrodes with the same preheat treatment. The results indicate that weldments made with these electrodes in the as-welded condition were equal to those fabricated with E6020 electrodes and preheat treatment for the FK steel used in this investigation. The transition temperature was the lowest (−65° F) of any found in the tests with the web-hole type of splice.

11. Alternate fabrication procedures aiming to avoid the unfavorable effects of the web holes adjacent to the flanges have been suggested. Butt weldments made by continuous welding of flanges and web without holes require careful attention to the condition of the weld in the fillet region but this type of splice is entirely practical. A series of impact tests on beams with this type of splice, using E6020 electrodes for comparison with similar beams fabricated with web holes, show that the continuous weld splice of FK steel beams in the as-welded condition had a transition temperature of about −70° F which is 40° F lower than similar beams with web holes. Examination of the welds indicated some flaws at the flange-web weld junction, a condition which can be overcome by precautions in the welding operation. The test results indicate a decided improvement in low-temperature performance with this type of splice.

12. The investigation reported here started with limited objectives but, with the accumulation of data

and observations, the studies were extended to provide information dealing with fabrication and splice design. These by-products are a natural outgrowth of continuing study and themselves suggest the need for further investigation of the adequacy of welded-beam fabrication and beam splices. Other possible studies of interest to the designer include (1) optimum preheat temperatures particularly for thick materials; (2) influence of the properties and grade of steel on the effectiveness of different types of electrodes; (3) further study of the effect of hydrogen and moisture control of electrodes; (4) alternate designs of butt splices in beams; (5) resistance to fracture at low temperatures of built-up beams with heavy flanges and web-flange fillet welds.

ACKNOWLEDGMENTS

The authors wish to acknowledge the joint sponsorship of this investigation by the office of Naval Research and the Welding Research Council, which made this project possible. The advice and recommendations of the Advisory Committee is greatly appreciated. The interest and cooperation of LaMotte Grover, Chairman of the Structural Committee and William Spraragen, Director of the Welding Research Council, have been particularly helpful. We wish to thank the Bethlehem Steel Co. for its cooperation in the many details of materials and fabrication of beam specimens. Through the generous contribution of the Research Corporation to this investigation, the instrumentation used was made possible. Acknowledgment is due the members of our laboratory staff and especially Prof. E. C. Ingalls, formerly a member of the staff, for his contributions in the development of instrumentation and conduct of many of the tests.

References

1. Krefeld, W. J. and Ingalls, E. C., "Investigation of Beams with Butt-Welded Splices Under Impact," THE WELDING JOURNAL, **26** (7), Research Suppl., 372-s to 432-s (1947).
2. Krefeld, W. J. and Ingalls, E. C., "Residual Stresses in a Butt-Welded I-Beam," *Ibid.*, **27** (8), Research Suppl., 417-s to 420-s (1948).
3. "Cracking of Simple Structural Geometries," Progress Rept., Project SR-118, May 1952, Ship Structure Committee Contr. No. s-50250.

Appendix

Metallurgical Report submitted by Bethlehem Steel Co. for this project including melting and Mill Practice and Fabrication of Beams

PART I. CHEMICAL ANALYSIS (see Table 1 of Report)

PART II. MELTING PRACTICE

Procedure	*34J333*	*35J272*
Process	Basic open hearth	Basic open hearth
Materials charged:		
Limestone, lb	18,000	20,000
Iron ore, %	None	4.8
Cold scrap, %	53.4	34.5
Hot metal, %	46.6	60.6
Metallic charge, lb	258,300	286,960
Carbon at melt	0.58	1.50
Time: Charge to melt	9:20	7:10
Working materials:		
Iron ore, lb	7000	12,000
Time: Last ore addition to tap	1:03	2:20
80% FeMn, lb	None	1500
Roll scale, lb	1000	None
Limestone, lb	2000	None
Fluorspar, lb	500	500
Burnt lime, lb	None	1500
FeO: Prior to additions, %	13.6	12.5
Furnace additions:		
80% FeMn, lb	500	3500
Time: Melt to tap	1:13	3:35
Total time	10:33	10:45
Ladle additions:		
80% FeMn, lb	1000	None
50% FeSi, lb	200	1400
Aluminum, lb	None	270
Coal, lb	480	None
Ingot data:		
Mold additions: Aluminum, oz per mold	15	None
Size, in.	25 x 30 x 88	23 x 29 x 89
Design	Open top, big end down	Sinkhead, big end up
Condition of tops	Flat	
Sinkhead insulation	None	Slag wool
Weight, lb	15,860	13,300
Number made	15	19
Number applied	5	10
Time intervals:		
(*a*) Tap to teem, min	13	15
(*b*) Teem to charge in soaking pits, min	40	105
(*c*) In soaking pits, hr	7	5.5
Temperatures:		
(*a*) Ingots at draw, ° F	2230–2235	2200–2280
(*b*) Beams at finishing mill, ° F	1760–1780	1700–1800

PART III. MILL PRACTICE

Rolling Practice. All ingots were rolled bottom first. The ingots in each heat were numbered in the order of rolling. This also indicates the relative order in which they were poured, but not their position in the heats. On heat 34J333, ingots 1 through 5 correspond to ingots 5 through 9 of the 15 ingots poured. On Heat 35J272, ingots 1 through 10 correspond to ingots 5 through 14 of the 19 ingots poured.

Cutting Practice. Five 28-ft beams were cut from each ingot. Only the bottom five multiples of each ingot were applied to this order.

A 4-ft test piece was cut from the top portion of the bottom (*E*) cut of the third ingot rolled on each heat (ingot No. 7 on both heats).

Hot Bed Practice. The beams were placed on one hot bed (approximate capacity 100 beams) with the flanges toe to toe (web vertical). This is the conventional procedure for cooling beams of this section. Only one hot bed was utilized in cooling to enhance accuracy in identification.

Identification. Each beam was stamped on the flange directly above the web with the heat number, ingot number (order of roll) and cut number (*E* through *A*, bottom to top).

Straightening. The beams were gag straightened when cold to commercial tolerance.

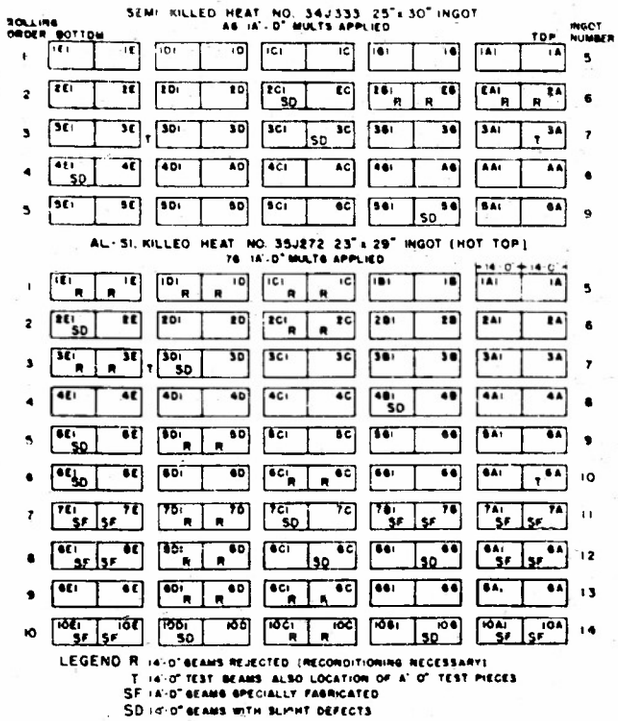

Fig. 26 Status of Beams—Columbia University Project

Inspection. All beams were carefully inspected for surface defects, laminations, straightness and length.

Piling. The *A*, *B*, *C*, *D*, and *E* cuts of each heat were piled in separate lifts and stored under cover for future use as requested by the Structural Steel Committee.

Figure 26 shows the status of each beam rolled for the Columbia University Project.

PART IV. FABRICATION OF BEAMS

Selection of Beams. The beams from Heat 35J272 were designated for special fabrication by the Structural Steel Committee of the Welding Research Council.* Following is the welding procedure used in the fabrication.

Filler Metal. Root Passes: $^5/_{32}$-in. diam AWS-ASTM E6011 welding rod. Subsequent Passes: $^3/_{16}$-in. diam AWS-ASTM E6020 welding rod.

Process. Arc welded.

Equipment. The supply of welding current was provided by a 500-amp, 25-cycle a-c transformer.

Position of Welding. Beams were mounted in a specially constructed positioning device. This permitted the beams to be rotated about their longitudinal axis so that welding could be done in the flat position.

Preparation of Base Metal. The web and flange surfaces to be joined by welding were beveled by machine flame cutting to the lines and dimensions shown on the Bethlehem Steel Co. Drawing No. DL-197-$^1/_4$ (see Fig. 7).

Tacking. The flanges were tack welded (about 1 in.) at four points as shown in Detail A, Fig. 27. The tacks were placed on the outer flange surface and were removed by gouging prior to placing Pass 3 as explained in the paragraph Flange-Joint Welding below.

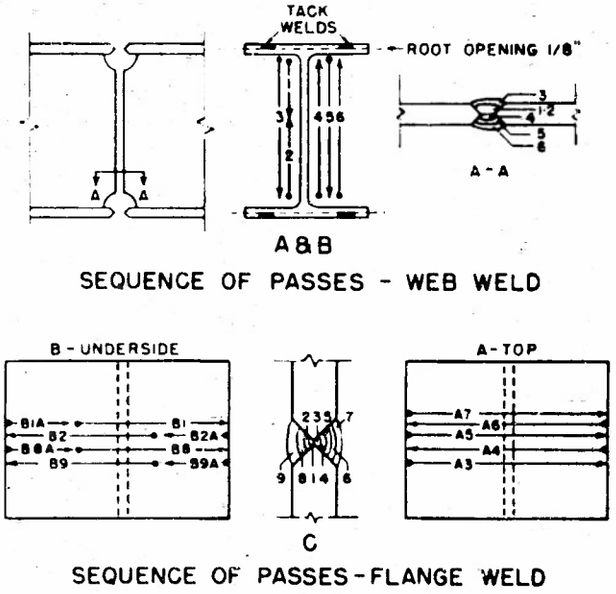

Figure 27

Web-Joint Welding. The web-joint was welded first, with one operator performing all the welding. The sequence and direction of welding is shown in Detail B in Fig. 27. Root passes 1 and 2 were made using a $^5/_{32}$-in. diam E6011 welding rod. Pass 3 which was made with a $^3/_{16}$-in. diam E6020 welding rod completed one side of the web joint. The beam was then rotated 180 deg. After back gouging to sound metal, Passes 4, 5 and 6 were made with the $^3/_{16}$-in. diam E6020 welding rod to complete the weldment.

The coped holes at each end of the web were hand burned back to assure sound metal at the end of the weld.

Flange-Joint Welding. The sequence and direction of welding is shown in Detail C in Fig. 27. Root Pass B1-B1A* was placed on the underside of the flange using the $^5/_{32}$-in. diam E6011 welding rod. Pass B2-B2A was then placed using the $^3/_{16}$-in. diam E6020 welding rod. The beam was rotated 180 deg and back gouged to sound metal. The outside of the flange was then completed by placing Passes A3, A4, A5, A6 and A7 with the $^3/_{16}$-in. diam E6020 welding rod. The beam was again rotated 180 deg and Passes B8-B8A and B9-B9A were made on the underside of the flange with the $^3/_{16}$-in. diam E6020 welding rod to complete the weldment. The same procedure was used in welding the opposite flange joint.

The overflow metal at each of the four flange-joint edges was back gouged to sound metal, welded and hand ground level with the flange edge.

Special Heating. Beams 7A and 8E were preheated

* Refers to first lot fabricated. Following procedure applies to all beams furnished

* Passes on the underside of the flange were made in two parts (Detail C, Fig. 27). For example: The first part of Pass 1 was made from the starting point toward the flange edge as indicated by the arrow *B1*. The second part of Pass 1 was made from the opposite flange edge to the starting point of *B1* as indicated by the arrow *B1A*.

and welded at an interpass temperature of 350° F (measured by Tempilstik). Beams 7A1 and 7E1 were stress relieved subsequent to welding and prior to shipment. The stress relieving consisted of heating to 1150° F, hold 2 hr, furnace cool to 500° F and air cool.

PART V

Results of physical tests made at the mill are included with data shown in Tables 2, 3 and 4.